UCRL-18459
cy. 2

University of California

Ernest O. Lawrence Radiation Laboratory

RECEIVED
LAWRENCE
RADIATION LABORATORY
OCT 21 1968
LIBRARY AND
DOCUMENTS SECTION

MASS SPECTROMETRIC STUDY OF PHOTOIONIZED GASES

Michael Mosesman
(Ph.D. Thesis)

September 1968

TWO-WEEK LOAN COPY

This is a Library Circulating Copy which may be borrowed for two weeks. For a personal retention copy, call Tech. Info. Division, Ext. 5545

Berkeley, California

UCRL-18459
cy. 2

DISCLAIMER

This document was prepared as an account of work sponsored by the United States Government. While this document is believed to contain correct information, neither the United States Government nor any agency thereof, nor the Regents of the University of California, nor any of their employees, makes any warranty, express or implied, or assumes any legal responsibility for the accuracy, completeness, or usefulness of any information, apparatus, product, or process disclosed, or represents that its use would not infringe privately owned rights. Reference herein to any specific commercial product, process, or service by its trade name, trademark, manufacturer, or otherwise, does not necessarily constitute or imply its endorsement, recommendation, or favoring by the United States Government or any agency thereof, or the Regents of the University of California. The views and opinions of authors expressed herein do not necessarily state or reflect those of the United States Government or any agency thereof or the Regents of the University of California.

UCRL-18459

UNIVERSITY OF CALIFORNIA

Lawrence Radiation Laboratory
Berkeley, California

AEC Contract No. W-7405-eng-48

MASS SPECTROMETRIC STUDY OF PHOTOIONIZED GASES

Michael Mosesman

(Ph.D. Thesis)

September 1968

CONTENTS

ABSTRACT

I. INTRODUCTION 1

II. APPARATUS 2

A. Light Source 2

B. Reaction Cell 7

C. Ion Injection Lens 9

D. Quadrupole Mass Spectrometer 12

E. Gas Handling System 16

1. Vacuum line 16

2. Mixture preparation 18

F. Gas Purity 20

G. Differential Pumping System 21

H. Experimental Difficulties 21

III. FACTORS WHICH DISTORT THE ION SPECTRUM 23

A. Instrumental 23

B. Sampling Process 23

IV. DATA TAKING AND REPORTING 25

A. Nomenclature 25

B. Apparatus Settings 25

C. Method Used to Obtain Intensities 28

D. Experimental Procedure 29

E. Photoionization Light Sources 29

V. EXPERIMENTAL RESULTS AND DISCUSSION 32

A. Photoionization of Nitric Oxide 32

B. Photoionization of Ammonia 37

V. continued

C. Photoionization Dimethylamine 41

1. Series I 43

2. Series II 62

3. Series III 63

D. Photoionization of Trimethylamine 69

1. Series I 71

2. Series II 73

E. Photoionization of Methylamine 80

VI. THERMODYNAMIC DATA 85

VII. CONCLUSIONS 88

ACKNOWLEDGEMENTS 90

REFERENCES 91

MASS SPECTROMETRIC STUDY OF PHOTOIONIZED GASES

Michael Mosesman

Inorganic Materials Research Division, Lawrence Radiation Laboratory
and Department of Chemistry
University of California, Berkeley, California

ABSTRACT

The ionic composition of gaseous photoionized nitric oxide, ammonia, methylamine, dimethylamine, and trimethylamine has been studied. The photoionized gases were sampled through a very small leak and analyzed with a quadrupole mass spectrometer. The leak consisted of thirty holes, the diameter of which was 0.010 mm. The holes were laser drilled in 0.0038 mm thick platinum foil. The pressure range studied extended from 0.030 to 10.0 mmHg. The only detectable ion in nitric oxide at 294K was NO^+. In ammonia and the amines many ions were detected at 294K. Some of these ions were attributed to ion-neutral association reactions. From a study of the temperature dependence of these reactions the corresponding enthalpies and entropies were derived.

I. INTRODUCTION

Frequently deionization processes such as ion-ion recombination, ion-electron recombination, or diffusion are studied without the benefit of the knowledge of what ions are actually involved in such processes. The obvious solution is to incorporate a mass spectrometer into the rate determining apparatus. In this case the ionized gas in which the rate process is measured serves as an ion source for the mass spectrometer. The initial stimulation for the present study came from a previous work[1] on the rate of loss of charge in photoionized nitric oxide at pressures in the tenths mmHg range diluted with inert gases in the mmHg range. In that work the ions were not investigated mass spectrometrically but simply collected. Crude mobility measurements indicated that a mass spectrometric study was necessary to identify with certainty what ions were recombining. In our study we simulate conditions under which the rate study was made and sample the photoionized gas to determine the ionic spectrum.

In addition, it was later realized that if any primary ions complexed with a neutral whose pressure could be controlled and if such complexing reached equilibrium, the enthalpy of the complex could be determined if the equilibrium could be followed as a function of temperature.[2-8] This follows from the equation

$$K(p) = e^{-(\Delta H - T\Delta S)/RT} .$$

From the enthalpy one can then estimate the bond energy of the complex.

An apparatus was built to accomplish these two objectives.

II. APPARATUS

The apparatus that was built to determine the ionic composition and to perform the equilibrium measurements in a photoionized gas consisted of the following items: a photoionization light source, a photoionization cell capable of temperature control, a vacuum preparation and admittance system, a very small leak, an electrostatic ion injection lens capable of ion modulation, a quadrupole mass spectrometer, a differential pumping system, and ion detection instrumentation. Figure 1 shows the experimental layout of these items. Figure 2 is a block diagram of the apparatus and the essential electronic equipment.

A. Light Source

The ultraviolet light used to photoionize the gases studied was emitted from a microwave discharge of an inert gas. The microwave source was a QK-60 magnetron operating at a power input of 100 watts. The magnetron output was coupled to a Broida[9] cavity with a flexible microwave cable. The discharge was contained inside a 13 mm o.d. piece of quartz tubing with a 3.2 mm thick quartz flange on one end. As is shown in Fig. 3, this flange was used to attach the lamp via an O-ring to the vacuum chamber. One this end was sealed a 1 mm thick LiF window with a silver ring and AgCl cement. The window, in principle, could have been sealed directly to the quartz but, in practice, this procedure was found unsatisfactory. The silver ring was easily sealed to the quartz and to the LiF window with AgCl and therefore was used to facilitate the assembly. (See Fig. 4.) The ionizing light produced in the discharge passes through the window, into the main vacuum chamber, and through another LiF window attached to the photoionization cell.

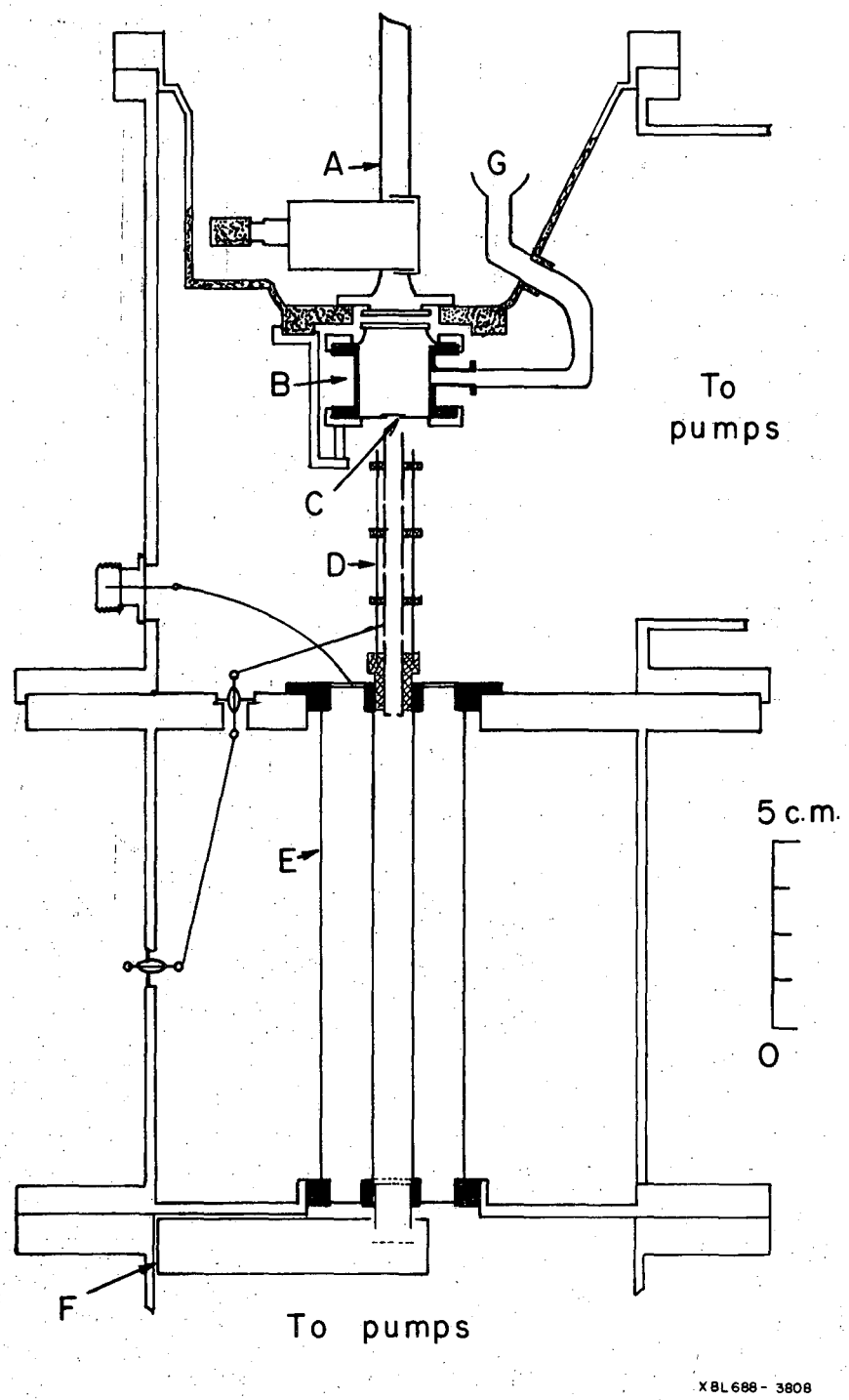

Fig. 1 Experimental layout.
(A) Lamp, (B) Reaction cell, (C) Sampling leak, (D) ion lens, (E) Quadrupole mass spectrometer, (F) Magnetic electron multiplier and (G) To gas handling system.

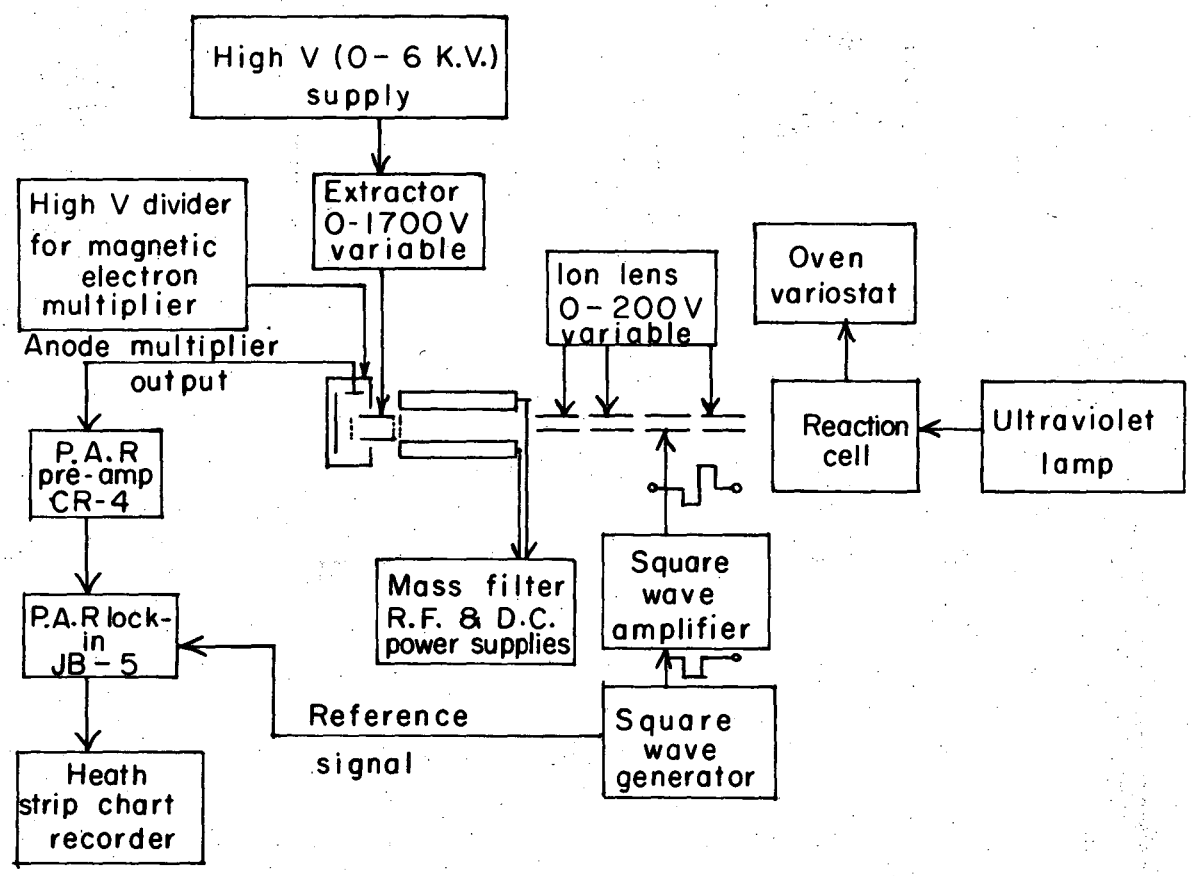

XBL 688-3820

Fig. 2 Block diagram of experimental setup

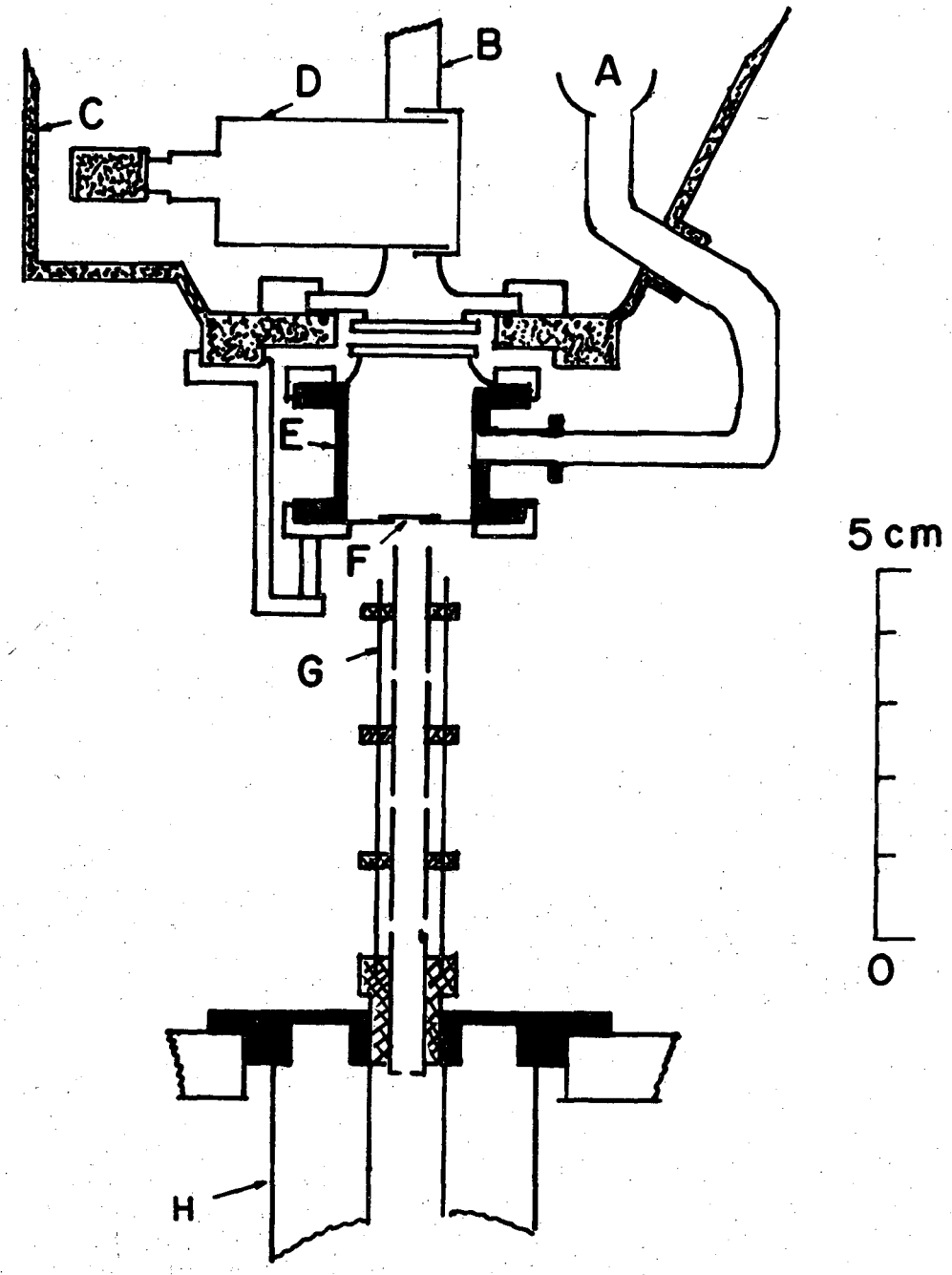

XBL688-3803

Fig. 3 Detail of ion source. (A) To gas handling system, (B) quartz lamp, (C) flanged cone, (D) Broida cavity, (E) reaction cell, (F) sampling leak, (G) ion lens, and (H) quadrupole mass spectrometer.

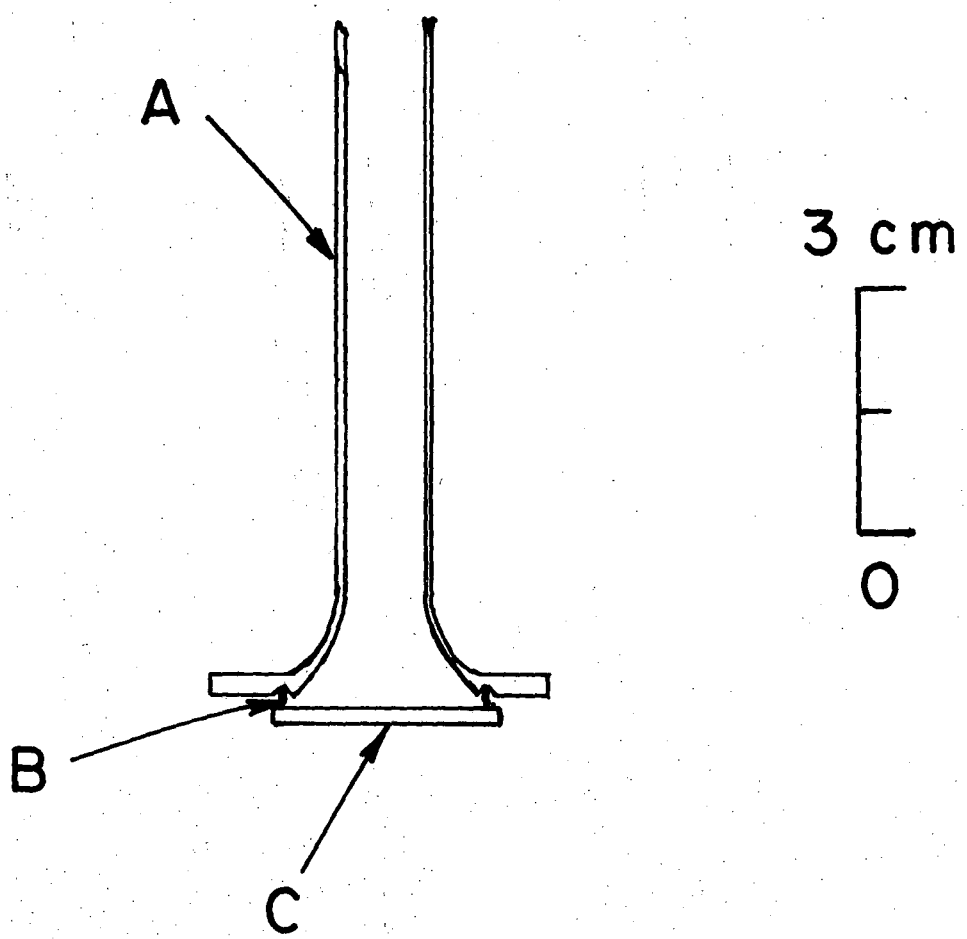

XBL688-3789

Fig. 4 Detail of lamp construction:

A. Quartz tube
B. Silver ring (Drawing LRL 12M880)
C. Lithium fluoride window

In order to avoid the many lined emission spectrum of water desorbed from the walls of the quartz by the action of the discharge, the lamp was fitted with a cold finger. When krypton and argon were discharged, the finger was cooled with liquid nitrogen; when xenon was employed, solid CO_2 was used as the coolant.

The pressure of the rare gases at which the emission lines were most intense have been shown by Okabe[10] to be around 1 mmHg. Accordingly Kr was used with its pressure that at liquid nitrogen temperature, Ar at 1 mmHg, and Xe at 0.75 mmHg.

In some respects the lamp arrangement was unsatisfactory. The ultraviolet light was beamed directly into the sampling pinholes. Some of the light which passes through the pinholes traveled all the way to the magnetic electron multiplier and was detected as noise. Also if the light were beamed horizontally across the pinholes, it would have been interesting to make observations on the effect of producing ions at given distances away from the pinholes.

B. Reaction Cell

The reaction cell was fabricated from stainless steel type 304 and was flanged with knife edges. The LiF window through which the ultraviolet light entered was sealed to a silver gasket with AgCl cement. The 0.0038 mm thick platinum foil was rolled from 0.0064 mm thick stock. It was cemented to a flat silver gasket and then shipped to Maser Optics in Boston, Mass. The foil always tended to wrinkle slightly in the cementing process. At Maser Optics thirty 0.010 mm maximum diameter holes were laser drilled in the foil. The pattern of the holes was five rows of

6 holes with 0.076 mm between the holes. The pattern was successfully drilled within 0.076 mm of center of the flat silver gasket. These silver gaskets were then carefully compressed on the knife edged flanges to provide a vacuum tight assembly. Although the knife edges were designed to shear the silver gaskets, the compression process tended to cause the platinum foil to wrinkle slightly.

The design of the cell and the assembly procedure for compressing the flat gasket on the knife edge was performed in such a manner to keep the pattern of pinholes concentric with respect to the perimeter of the compression flanges. The reaction cell was then assembled to the flanged cone with a device (cell centering jig) such that the reaction cell compression flanges were concentric with the mating surfaces of the flanged cone.

The reaction cell was fabricated with a glass-kovar seal welded onto its side. While the reaction vessel was being held concentrically on the flanged cone, a glass blown joint was made connecting the glass-kovar seal to a piece of glass sealed by epoxy cement into the side of the flanged cone. The cell centering jig was removed and a support 180° from the glass-kovar seal was attached. The support had 3 jacks with glass tubing spacers between each jack and the bottom compression flange. The cone was then taken to a jig borer where the jacks were adjusted to make the inside surface of the bottom cell compression flange parallel with the corresponding mating surface on the flanged cone. When the flanged cone was placed on the apparatus, the pattern of the sampling holes would be on the same axis as the ion injection lens and the quadrupole mass spectrometer (see Fig. 3).

The reaction cell as described above was mounted so that it was electrically and thermally isolated. An insulated nichrome heating element was wound around the reaction vessel to thermostat it at temperatures above 20°C. In order to cool the cell to below room temperature, copper wires were wrapped around the cell and then pressed against a cold finger with a few strips of teflon tape between the wires and cold finger for electrical insulation. With the cold finger filled with liquid nitrogen, the cell could be cooled to -70°C in about 6 hours. An arrangement was set up so that the cold finger could be filled automatically at fixed time intervals. Temperatures intermediate between -70°C and 20°C were obtained by using the oven in conjunction with the cold finger.

Chromel-Alumel thermocouple wires of 0.076 mm diameter were spot welded to the cylindrical outside surface of the reaction cell. To determine how well such a thermocouple monitored the gas temperature, an additional thermocouple was inserted inside the reaction cell. With a mmHg of gas in the cell, there was no detectable difference between thermocouple readings at any of the temperatures investigated.

One additional wire was attached to the cell to float it at the desired electrical potential. This was about +1.5 volts for positive ions. The cell was floated at a positive voltage so that positive ions would have enough energy to enter the quadrupole mass spectrometer.

C. Ion Injection Lens

The ion lens (see Fig. 3) served to transport the ions as they emerged from the sampling pinholes into the quadrupole mass spectrometer. The lens consisted of four cylindrical tubes. The first two and the

last two were essentially two electrostatic lenses in series. The lens system was designed from data given by Spangenberg.[11]

Crude attempts to determine the transmission efficiency of the lens were unsuccessful. However we can estimate the total diminution of ion intensity as the ion current travels to the magnetic electron multiplier (MEM). The ion density in the photoionized gas was estimated to be 10^9 ions/cc.[12] The ion current coming from the sampling pinholes was Fn where F was the conductance of the pinhole in cc/sec and n was the ion density. For viscous flow in air F = 20 A liters/sec where A = cross section area of the orifice in cm^2. $A = 2.4\times10^{-5}$ cm^2 for the thirty 0.010 mm diameter sampling holes. Then $Fn = (0.47 \text{ cc/sec})\times(10^9 \text{ ions/cc}) = 10^9$ ions/sec which was equivalent to a current of 10^{-10} amp.. With the gain of the magnetic electron multiplier estimated to be 10^6, a 10 mv output at the lock-in amplifier corresponded to a primary current of 10^{-16} amp at the MEM. A typical experiment in nitric oxide resulted in a 200 mv total ion signal which corresponded to 10^{-14} amp. This calculation shows that the primary ion intensity issuing from the sampling orifice had been diminished by 10^{-4}.

Nominal working voltages used on the four ion lens elements were respectively -20, -70, -64, and -24 volts. Actually a square wave voltage, -70 to + 70 voltags peak to peak, at a frequency of 100 cps, was applied to the second lens element. This voltage served to modulate all the ions which entered the quadrupole mass spectrometer. This ion modulation then made possible the use of phase sensitive detection of the amplified MEM output. The amplifier used to provide the square wave of variable voltage and frequency is shown in Fig. 5.

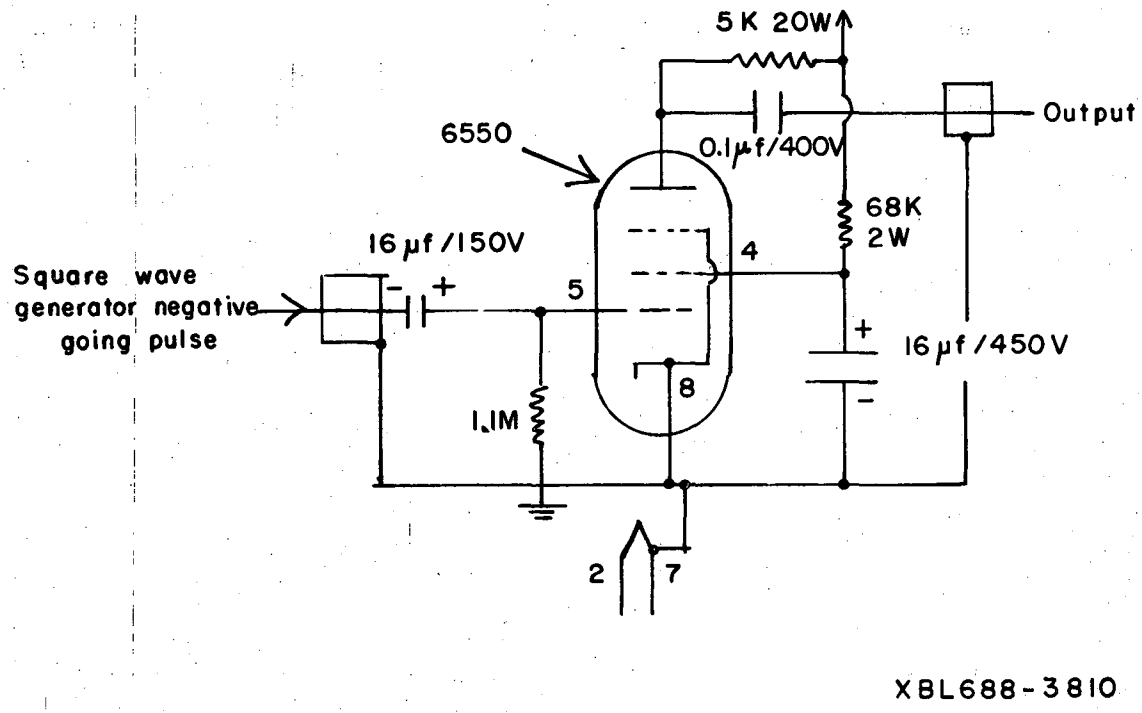

Fig. 5 Square wave amplifier used to modulate ion current.

We used a phase sensitive detection method because the direct current signal/noise ratio made it impossible to measure some mass resolved ion currents. The main source of noise came from the ultraviolet light emitted by the discharge. Some of this light exited the sampling pinholes. It then traveled to the cathode of the magnetic electron multiplier where it ejected photoelectrons.

The last lens element protrudes into the R.F. field of the mass spectrometer. A small flange with an aperture in it was spot welded to the end of this lens element. This aperture was one variable which determined the performance of the mass spectrometer. Its diameter, 1.6 mm, was chosen to give a compromise in resolution and intensity. A better arrangement with regard to the performance of the mass spectrometer might have been achieved by placing the aperture in a plate at ground potential. This plate would serve to shield the quadrupole from the lens voltages. It might also permit the ions to enter the quadrupole with a smaller angular spread.

D. Quadrupole Mass Spectrometer

The quadrupole mass spectrometer[13] (see Fig. 6) was a resonance type of instrument. Ions which were stable in the spectrometer underwent helical paths and exited with fairly high radial velocities. Unstable ions also underwent helical orbits but the radius of the orbits rapidly increased until these ions were neutralized on the poles.

The parameters which determined which ions were stable in the quadrupole were the frequency and absolute value of the R.F. voltage applied to the poles, the D.C. voltage the R.F. rides on, the aperture into the quadrupole, and the inscribed radius of the quadrupole. The latter was fixed and

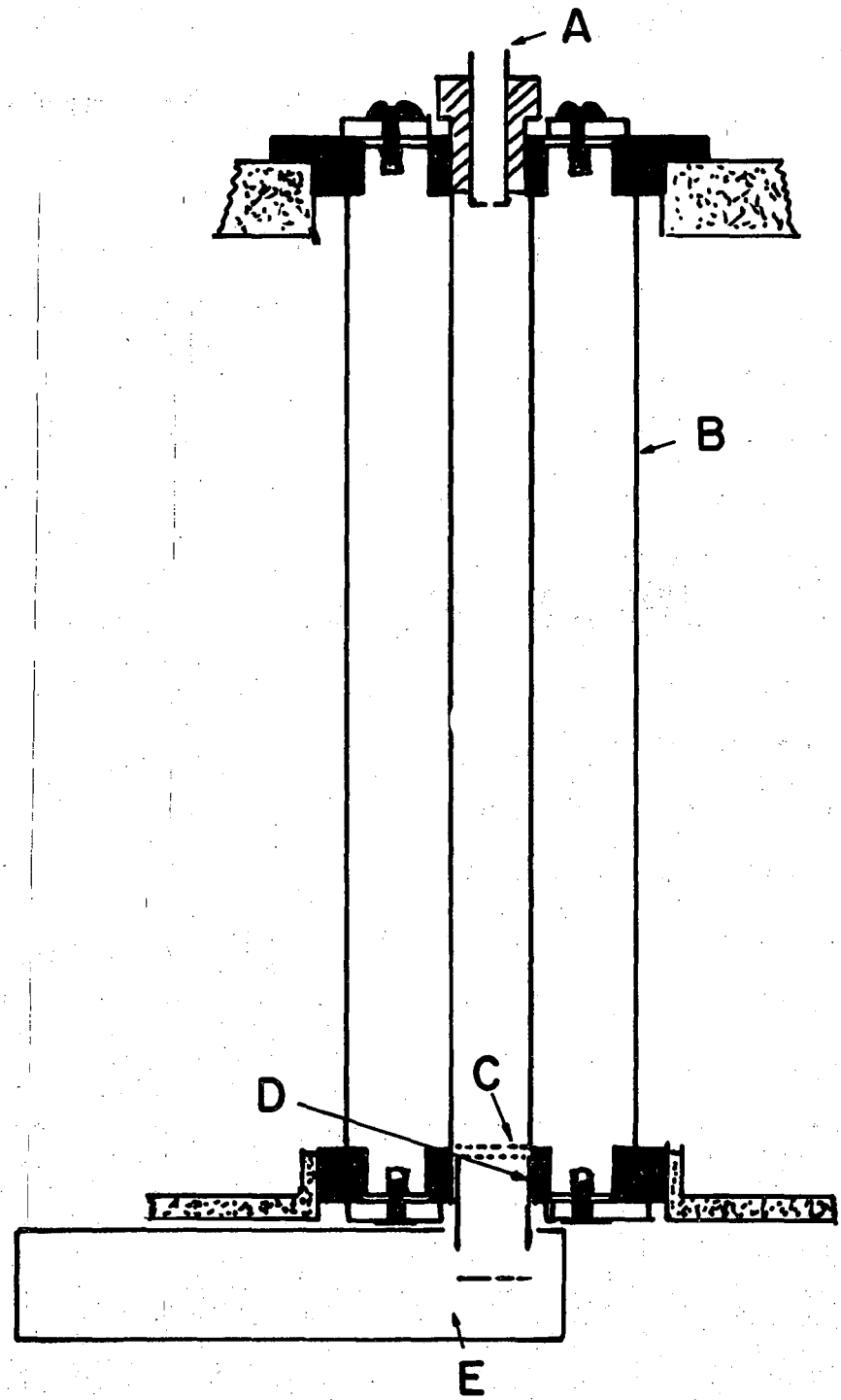

XBL688-3805

Fig. 6 Detail of quadrupole mass spectrometer. (A) Last ion lens element, (B) quadrupole mass spectrometer, (C) grid over ground plate, (D) extracting tube, (E) magnetic electron multiplier.

therefore not an experimental variable. The R.F. voltage could be varied from 50 to 500 volts peak at 4 different frequencies to cover the mass ranges 1 to 10, 3 to 30, 10 to 100, and 30 to 300. The electronics for generating the R.F. voltages and the poles and pole spacer design were essentially those used by Kent Wilson.[14] The voltage (Acos(wt) + B) was applied to diagonal poles with the same voltage of opposite sign being simultaneously applied to the other two poles. The ratio of the D.C. voltage, B, to the peak R.F. voltage, A, was called the D.C. bias. This ratio and the aperture size determined the mass resolving power with other parameters held fixed and with the initial radial velocities within certain limits. A mass scan was performed by keeping the D.C. bias constant and changing the absolute value of A and B. An 1/5 r.p.m. Bristol clock motor was attached to the helipot which varied the absolute values of A and B to provide a semiautomatic mass scanning facility.

The performance of the mass spectrometer fell into two categories. At low resolution all the stable ions which entered the quadrupole exited it. In such a situation a mass scan gave a trapezoidal signal shape for a stable ion. As the D.C. bias was increased the spectrometer reached a point where the transmission was not complete. The signal shape of a mass scan of a stable ion was then triangular.

Some of the stable ions which exited had large radial velocities. In order to minimize the loss of such ions, they were extracted rapidly with a high negative voltage. Also the path length from the end of the quadrupole field to the cathode of the magnetic electron multiplifer was made as short as possible. Initially the ions were simply extracted by extending a tube at -1700 voltage just past the bottom ground plate. The

ground plates, one at the top and bottom of the mass spectrometer, served to intercept stray ions that might hit the quadrupole spacers and build up an undesirable surface charge. Under all D.C. bias settings the signal shape of a mass scan of an ion was highly irregular. Upon placing a 96% transparency section of gold gauze over the ground plate, positioning the extracting tube about 1.6 mm away from the ground plate, and putting a piece of 96% transparency gold gauze on the end of the extracting tube, the mass scanned signal shape became highly regular. At low resolution settings the peak shape was trapezoidal and became triangular at higher D.C. bias settings.

The mass spectrometer exhibited one type of behavior which was not understood. This was that with a fixed D.C. bias, the measured resolution increased as a function of mass. This was true even when the resolution setting was such that trapezoidal peak shapes were obtained. The D.C. bias was measured at a fixed instrumental setting as a function of peak R.F. voltage and found not to vary. For example, at the same resolution setting, $m/\Delta m$ at mass 30 was measured to be 11 and at mass 60, was 13. It was still assumed that trapezoidal peak shapes meant the transmission of the quadrupole was 100%. This was because the peak ion intensity was constant as the D.C. bias was increased until a value of the bias was reached beyond which the peak intensity dropped off sharply.

It was of interest to determine how well the observed performance compared to design expectations. Using Paul's[13] equation (18) with the ratio D.C. voltage/peak R.F. = 0.1635, one calculates the resolution, $m/\Delta m$, to be 30 (Δm is the width of the peak at the base of signal).

Experimentally it was measured to be 11 at mass 30. The maximum achievable resolution should depend on the ion injection aperture size and the initial radial ion energies. The aperture size was 1.6 mm which according to Paul's equation (21)[13] should give an achievable resolution of 23. Actually resolutions of the the order of 60 could be achieved but with an accompanying sacrifice in ion intensity.

Ions which were extracted from the mass spectrometer impinged on the cathode of a Bendix type 306 resistance strip magnetic electron multiplier.[15] Crude measurements indicated this detector produced gains of the order of 10^6 with sensitivities to ions different in mass by a factor of two varying roughly from 5 to 10%. Working voltages for detecting positive ions with the multiplier were these: Field strip input end = -800 volts, field strip output end = 0.0 volts, dynode strip input end = -1700 volts, dynode strip output end = -170 volts, and, anode $\cong$ 0.0 volts.

The current drawn from the anode of the magnetic electron multiplier was passed through a 10M ohm resistor. The voltage produced then was put into a Princeton Applied Research Corporation low noise amplifier model no. CR-4. Its output was fed into a P.A.R. lock-in amplifier model JB-5. The output from the JB-5 was put into a Heath strip chart recorder.

E. Gas Handling System

1. Vacuum Line

A conventional vacuum line (see Fig. 7) was built to distill the gases studied, to admit them in a regulated fashion to the photoionization cell, to prepare mixtures of the photoionizable and inert gases, and to fill the photoionization lamp. The line was fabricated from glass and greased stopcocks. Granville-Phillips needle valves were used for pressure

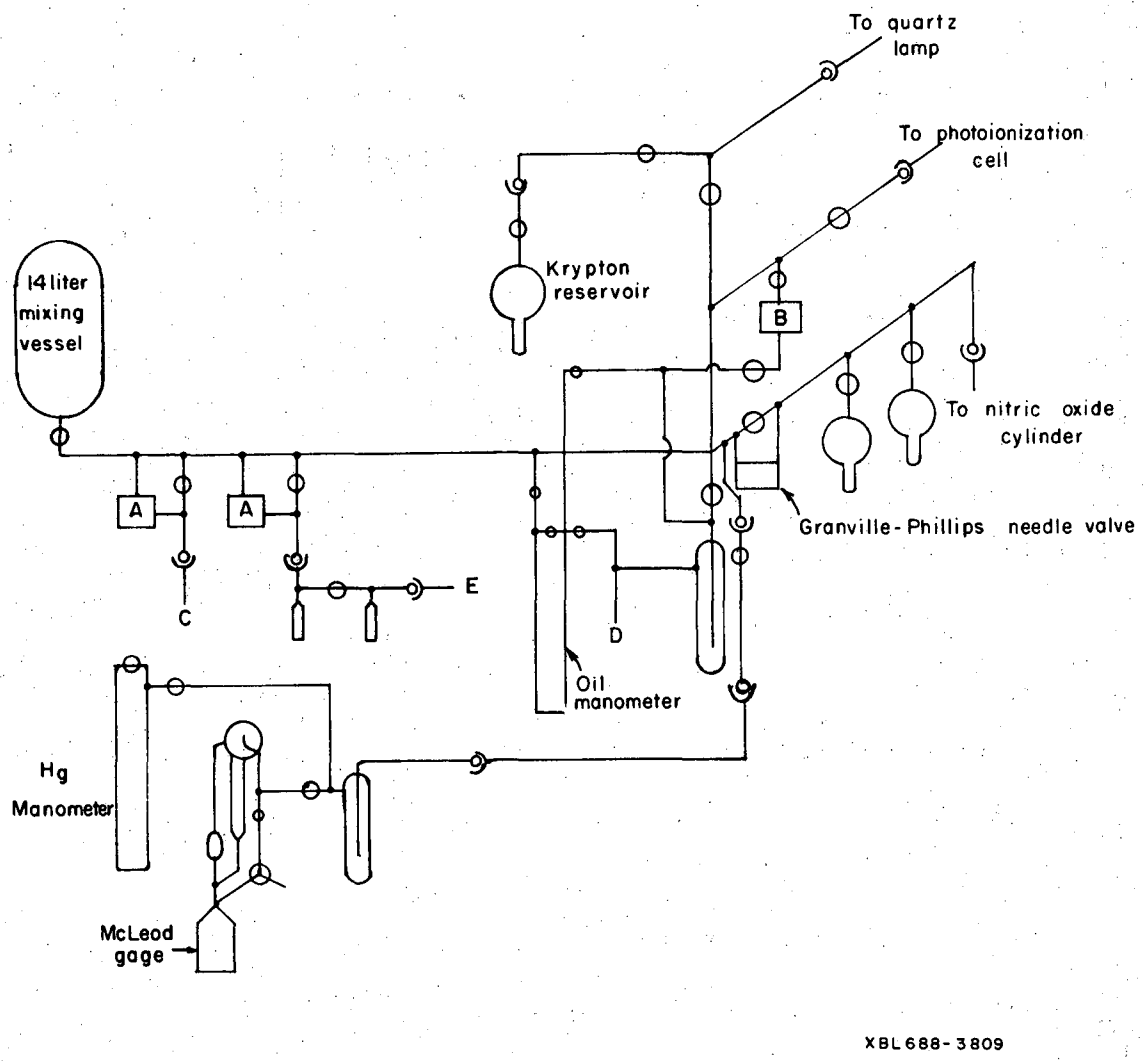

Fig. 7 Gas handling system. (A) Granville-Phillips needle valve, (B) capacitance manometer sensing head, (C) to cylinder of inert gas, (D) to small oil diffusion pump, (E) to ammonia or amine cylinder.

regulation. The line was evacuated with a 2 in. C.V.C. metal oil diffusion pump. The line could be evacuated to 10^{-6} mmHg with a trap between the diffusion pump and the system cooled to liquid nitrogen temperature.

Connection of the vacuum line to the reaction cell was accomplished with ball joints. A similar coupling including a section of stainless steel bellows was used to attach the lamp housing to the line.

2. Mixture Preparation

The preparation of mixtures containing the photoionizable gas at a pressure of the order of 0.10 mmHg mixed with an inert gas at about 10.0 mmHg initially posed a mixing problem. In order to obtain a homogeneous mixture, the following procedure was used. A 14 liter pyrex tube served as the mixing vessel. The volume of 14 liters was chosen by estimating what volume would be necessary so that the total pressure would be reduced by only 4% in 10 minutes as the gas effused through the sampling pinholes. The mixing vessel was evacuated, the stopcock to reaction vessel closed, and the photoionizable gas let in to the desired pressure which was read on a Granville-Phillips capacitance manometer. The manometer could detect pressures from 5 microns to 10 mmHg directly. The stopcock isolating the mixing vessel was then closed and the remaining gas pumped away. The vacuum line was then opened to a McLeod gauge with a liquid nitrogen cooled trap separating it from the rest of the system. Some inert gas was let in until the capacitance manometer gave the same reading as before. The pressure was measured with the McLeod gauge and it corresponded to the pressure of the photoionizable gas in the mixing vessel. In principle the capacitance manometer could have been calibrated at these low pressures but the 0-drift of the instrument made such a calibration inaccurate.

The gas was then pumped away, stopcocks to the capacitance manometer and McLeod gauge closed, and the stopcock to the Hg manometer opened. Then the inert gas was let into the line at a high enough pressure as indicated by the Hg manometer, so that upon expansion into the mixing vessel, the desired total pressure would be obtained. The stopcock to the mixing vessel was opened and the inert gas rushed in as a plug. The total pressure reached equilibrium in a few seconds as measured by the Hg manometer and then the stopcock was closed. The mixing vessel was warmed on one side with a hot air blower for five hours so that mixing would be accelerated via convection. The mixture was allowed to cool to room temperature and further mix over night.

The remaining gas in the line was evacuated, the Hg manometer isolated, and stopcocks to the reaction cell and the capacitance manometer reopened. If the capacitance manometer was exposed to pressures over 50 mmHg, recalibration would have been necessary. The reaction cell was always isolated during preparation of a mixture for obvious reasons.

When the reaction vessel had reached the desired temperature, the photoionization lamp was turned on. After a few minutes the mixture was let into the cell. The mass spectrometer signal of the primary photo-ion leveled of in about 5 minutes indicating that the gaseous mixture in the cell was homogeneous. If the pressure of the mixture was less than 10 mmHg, it was read directly with the capacitance manometer which had been calibrated in this pressure range with an oil manometer. If the pressure was greater than 10 mmHg, a static amount of gas could be admitted to the reference side of the capacitance manometer. The total pressure was then the reference pressure which was measured with an oil manometer plus that read on the capacitance manometer.

F. Gas Purity

The photoionizable gases were purchased from Matheson. Matheson's stated maximum impurities of these and the inert gases are given in Table I. Nitric oxide was cooled to liquid nitrogen temperature and pumped on to remove noncondensables. It was then twice distilled from a trap at liquid oxygen temperature to one at liquid nitrogen temperature. Dimethylamine freed of noncondensables at -196°C was singly distilled from a trap cooled with a toluene slush bath (-95°C) to one cooled with liquid nitrogen. Ammonia, methylamine, and trimethylamine were frozen to -196°C and removed of noncondensables. The inert gases were taken from cylinders and used without further purification. The tubulation up to the cylinder valve including the pressure regulator was evacuated prior to opening the cylinders.

Table I. Gas purity

Nitric Oxide	98.50%	Ammonia	99.95%	Methylamine	98.0%
Nitrous Oxide	0.45%	Water	45 p.p.m.	Dimethylamine	0.8%
Nitrogen Dioxide	0.20%	Oil	5 p.p.m.	Trimethylamine	0.6%
Nitrogen	0.20%			Water	0.8%
Dimethylamine	99.0%	Trimethylamine	99.0%	Helium	99.997%
Trimethylamine	0.3%	Methylamine	0.1%	Nitrogen	99.999%
Methylamine	0.3%	Dimethylamine	0.4%		
Water	0.4%	Water	0.5%		

G. Differential Pumping System

The vaccum chamber (see Fig. 1) into which the photoionized gas escaped must be kept at a low pressure. This was necessary to prevent serious loss in ion intensity from scattering processes and distortion of the ion spectrum due to reactions past the sampling pinholes. An N.R.C. 1500 liter/sec oil diffusion pump suitably baffled and valved was chosen to evacuate the effusing neutrals. With no gas in the reaction cell a background pressure of 3×10^{-7} mmHg could be achieved. With 10 mmHg of nitrogen in the reaction cell, an ion gauge on the side of the first chamber read 1.4×10^{-5} mm Hg. The pressure was undoubtedly somewhat higher inside the ion injection lens. The quadrupole mass spectrometer chamber was also pumped by a 1500 liter/sec oil diffusion pump similarly baffled and valved.

The diffusion pumps were suitably plumbed so that one mechanical pump could back both diffusion pumps when there was no gas load from the photoionization cell. A small vacuum solenoid valve was put in parallel with the main mechanical pump isolation valve. Under standby operation both diffusion pumps could be backed through this solenoid valve. In case of power, cooling water, or vacuum failure the solenoid valve closed and the diffusion pumps were turned off. This arrangement effectively prevented any serious oil contamination problems.

H. Experimental Difficulties

In the ammonia study, the light emitted from the argon lamp caused the lamp window to become seriously color-centered. When this occurred, the transmission of light through the window fell. Correspondingly, the ion intensities fell, and this made the measurement of ion intensities

difficult. The transparency of the lamp window could be recovered by bleaching it with a mercury lamp but this necessitated removing the lamp from the apparatus and consequently letting the apparatus up to atmospheric pressure.

The resolution of the mass spectrometer was satisfactory for the nitric oxide study, marginal in the ammonia, and unsatisfactory in some cases in the amine study. The obvious remedy would be to replace the 1.6 mm aperture into the quadrupole with a smaller one.

III. FACTORS WHICH DISTORT THE ION SPECTRUM

A. Instrumental

The resolution of the mass spectrometer under most of the experiments performed was high enough so that the current of an ion entering the spectrometer would be attenuated. The attenuation was inversely proportional to the resolution. The experimentally measured resolution was observed to increase slowly as a function of increasing mass. This effect served to decrease the heavy to light ion ratio.

Another possible source of distortion was the degree to which the gain of the magnetic electron multiplier depended on the mass of the impinging ion. This effect was expected to be small as intensity ratios were measured for ions differing in mass at most by a factor of two. The gain might be expected to increase slowly with increasing ion mass.

The two effects tended to cancel each other and the total distortion might be expected to be less than one order of magnitude. Since these effects were independent of the conditions in the ionization cell they should not affect the estimation of the enthalpy from a lnK vs. 1/T plot. The evaluation of the entropy would be affected.

B. Sampling Process

The condensation of neutral molecules around ions after they have passed through the sampling pinholes could be a serious source of distortion of the true ion spectrum. This effect should become important when the gas flowed through the sampling pinholes in a viscous manner.

Viscous flow was expected to occur when the ratio of the mean free path to the diameter of the pinhole became less than 1. The mean free path of helium at 10 mmHg and 300K was 0.014 mm, of helium at 10 mmHg and 200K was 0.010 and of ammonia at 1 mmHg and 300K was 0.036 mm. The diameter of the sampling pinholes were 0.010 mm. As will be shown in Section V, equilibrium constants were independent of the total pressure in mixtures of the photoionizable gases and helium. Also the equilibrium constant decreased as the proportion of the amine was increased. Both these observations indicated that condensation effects were not important.

It was also of interest to know from what region in the reaction cell the photoionized gas was being sampled. Kebarle[16] has shown that at pressures of from 5 to 20 mmHg, the bulk of ions formed by alpha particle irradiation of ammonia and ethylene came from " a 1 mm radius volume directly above the leak."

IV DATA TAKING AND REPORTING

A. Nomenclature

In the tabulation of results equilibrium constants are expressed for the association reaction to produce a complex. The units are $(mmHg)^{-1}$. Conversion of the equilibrium constants to units of cc/molecule at 20.0C can be accomplished by multiplying the equilbrium constant $K_{0,1}$ for the reaction

$$A^+ + B + B = AB^+ + B$$

is

$$K_{0,1} = \frac{(AB^+)}{(A^+)p(B)} \quad (mmHg)^{-1}$$

where p(B) is the pressure of B in mmHg.

We report all our results as equilbrium constants. In several cases the data indicate that true equilibrium has not been reached. In such a situation the figures for the "equilibrium constant" actually give just a steady state ratio.

B. Apparatus Settings

The voltages on the cell and the ion injection lens were the same for all of the data reported. Typical values of these voltages were given in Section II (C). The instrumental resolution setting for the nitric oxide experiments was 8.8. This setting, the D.C. bias, governs the ratio of the D.C. voltage to peak R.F. voltage applied to the poles of the quadrupole mass spectrometer. As the setting is raised the mass spectrometer will reach a point at which it does not transmit all of the ions in the mass range for which the quadrupole is tuned. At the

TABLE II.

Experimentally Measured Resolution

Resolution Setting Ion Mass	8.8 $m/\Delta m_b$ [a]	9.2 $m/\Delta m_b$	9.2 $m/\Delta m_h$ [b]
30[c]	11.	22.	
60[c]	13.	32.	
45,46[d]		10.	18.
59,60[d]		10.	20.
91[d]		17.	26.
119[d]		113.	31.

a. Δm_b refers to the width of the ion signal at its base.

b. Δm_h refers to the width of the ion signal at half its peak height.

c. Mass range was 10 to 100.

d. Mass range was 30 to 300.

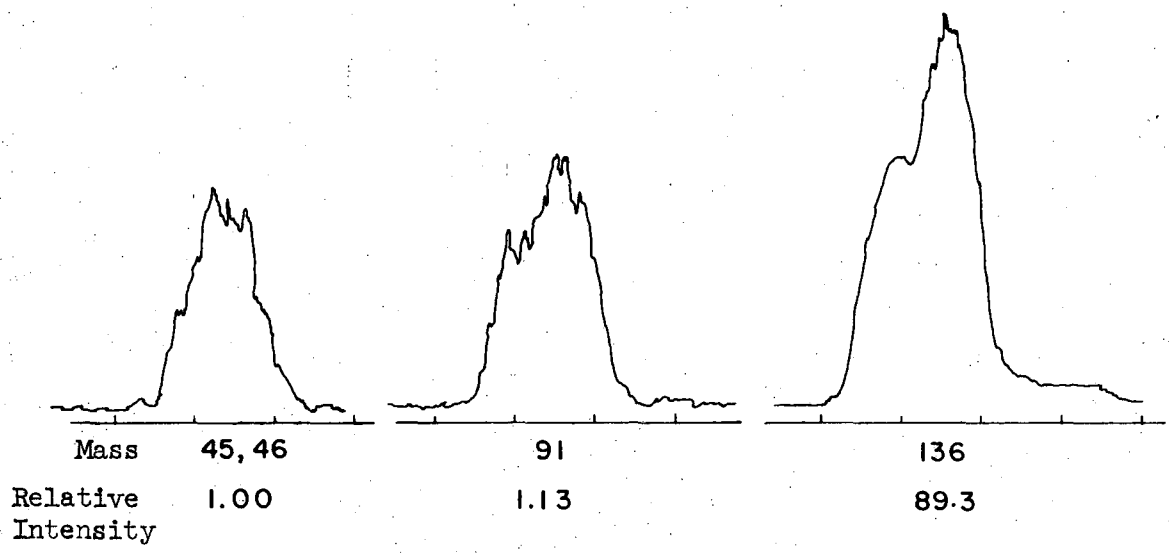

XBL 688-3788

Fig. 8. Typical mass spectra of Series I in dimethylamine. Experimental conditions: 1.45 mmHg amine, 20.0°C, Kr-Lamp. Each hash mark corresponds to 3 mass units.

8.8 setting the transmission is close to 100% as infered from the signal shape of a mass scan. Some of the data in the ammonia study were taken at a resolution setting of 9.2. Here the signal shape of a mass scan was triangular and therefore the transmission was less than 100%. In this case the percent transmission of an ion current through the quadrupole was dependent on its mass. This affects only the value of the entropy determined from a lnK vs. 1/T plot. All the data were taken in the amine studies with a resolution setting of 9.2.

Examples of the experimentally measured resolution as a function of the resolution setting are given in Table II. Typical mass spectra, Series I in dimethylamine, are shown in Fig. 8.

The magnetic electron multiplier was run with -1700 volts applied to the dynode strip input end and also to the extractor tube except during the trimethylamine study. Here the gain was lowered by reducing the above mentioned voltage to -1600 volts.

C. Method Used to Obtain Intensities

Ion intensities in the nitric oxide study were determined by setting the mass spectrometer to a fixed mass setting and measuring the intensity. The noise was measured at a mass setting where there was no ion signal. The difference between the signal at the fixed mass number setting and the noise was taken to be the measure of the ion intensity. This procedure was justified when there were no ion signals interfering with the signal of interest and when the signal shape of the mass scan was flat at the maximum. In the ammonia study some data were were taken like this. The rest were taken by performing a mass scan.

The difference between the maximum signal in the scan and that at the base of the peak where no ion signal was detected was taken to be representative of the ion intensity. All the data reported in the amine study were taken in this fashion.

D. Experimental Procedure

The reaction cell was thermostated to the desired temperature was described in Section II(B), page 9. All necessary electronics which were not already on standby were turned on. The discharge was ignited and the previously prepared mixture or the photonionizable gas alone was admitted to the reaction cell. Intensities were then measured with each signal usually being measured 3 times during the course of an experiment. The pressure of the photoionizable gas in the mixtures was corrected for the pressure drop upon expansion into the vacuum line and reaction cell. It was also supposed to decrease at the same rate as the total pressure. The spread in the data listed in the following tables and in the error bars on the graphs represented the experimental spread made during the course of an experiment. Systematic errors such as the pressure of the photoionizable gas and reproducibility of dial settings were estimated to be 20%; the reproducibility of a given experiment was estimated to be 30%.

The density of each gas was kept approximately the same at each temperature investigated. This procedure was followed so that distortions of the equilibrium constants due to different ion densities or to pressure effects would at least remain fixed.

The straight lines appearing in all the lnK vs. 1/T plots were

drawn visually. The data were not considered precise enough to merit a least squares treatment. Additional lines were drawn to estimate the spread in the enthalpy and entropy values reported. The entropy was calculated from the free energy equation.

$$R\ln K = -\Delta H/T + \Delta S$$

using the value of lnK obtained from the intersection of the straight line and the 294°K ordinate. The enthalpy is calculated from the slope of the straight line.

E. Photoionization Light Sources

For reference the photoionization lamps used with the various gases studied are given in Table III.

TABLE III

Ionization Potentials of the Gases Studied and the Energy of the Light Sources Employed

Gas	Ioniz. Pot. (ev)	Wavelength(A) Ioniz.Thresh.	Rare Gas	Emission Line(A)	Emission Line Energy(ev)
Nitric Oxide	9.25	1340.	Kr	1236.[b]	10.03
				1167.	10.64
Ammonia	10.15	1221.	Ar	1067.	11.62
				1048.	11.83
Methylamine	8.97	1382.	Kr	1236.	10.03
				1165.	10.64
Dimethylamine	8.24	1505.	Kr	1236.	10.03
				1167.	10.64
			Xe	1470.[b]	8.43
				1295.	9.57
Trimethylamine	7.82	1585	Xe	1470.	8.43
				1295.	9.57

a. Values taken from Ref. 17.
b. From Ref. 10, 1165 25% as intense as 1236; 1295 2% as intense as 1470.

It is important to know when the photoionization is non-uniform, that is, when the absorption of the ionizing light has become appreciable. The absorption cross sections for nitric oxide at 1236A and for ammonia at 1067A have been measured by Watanabe.[18] The absorption cross sections for dimethylamine and trimethylamine at 1470A were estimated from data given by Tannehbaum.[19] Table IV list these cross sections and the fraction of light absorbed at a pressure of 1 mmHg (3.29×10^{16} molec/cc), a path length of 2.54 cm and a temperature of 294K. The calculations indicate that absorption has become serious under these conditions.

TABLE IV.

Photoabsorption Cross Sections

Gas	Cross Section (cm^2)	Wavelength (A)	$I/I_o = e^{-\sigma c l}$
Nitric Oxide	2×10^{-18}	1236.	0.85
Ammonia	3×10^{-7}	1067.	0.085
Dimethylamine	1×10^{-17}	1470.	0.44
Trimethylamine	1×10^{-17}	1470.	0.44

V. EXPERIMENTAL RESULTS AND DISCUSSION

A. Photoionization of Nitric Oxide

The observations in the photoionization of nitric oxide fall into two categories, namely those under which complexes were observed and were absent. Initially experiments were conducted with mixtures of nitric oxide and helium or nitrogen. The photoionization of nitric oxide at a pressure of 0.130 mmHg diluted with helium at pressures from 5 to 2 mmHg at a temperature of - 0°C produced mass spectrometer signals indicating NO^+ had complexed with up to two molecules of nitric oxide. There were also signals of appreciable intensity at higher mass numbers which were not critically investigated. At room temperature, 20°C, under the same experimental conditions only NO^+ could be detected. Table V summarizes the observations.

The measured equilibrium constant for the dimerization was found to be independent of helium pressure in the pressure range 10 to 2 mmHg while the trimerization equilibrium constant showed a marked dependence, increasing three fold over the pressure range.

As the temperature was raised 36°C, $K_{0,1}$ increased very slightly and $K_{1,2}$ decreased fourfold. $K_{0,1}$ appeared independent of nitric oxide pressure while $K_{1,2}$ increased with decreasing nitric oxide pressure.

Experiments with nitrogen as the diluent at 10 mmHg gave equilibrium constants which were slightly larger than those with helium at -70°C. It was necessary to double the nitric oxide pressure to 0.260 mmHg to be able to make the measurements. When the temperature was raised by 70°C, $K_{0,1}$ appeared unchanged while $K_{1,2}$ had decreased by a factor of thirty. In experiment D^2 the discharge producing the ionizing radiation was moved next to the lamp window to see if the equilibrium constants were

Table V. Equilibrium constants measured in nitric oxide

$K_{0,1}$[a] $(mmHg)^{-1}$	$K_{1,2}$[a] $(mmHg)^{-1}$	Press. (mmHg) Nitric Oxide	Press. (mmHg) Diluent	Temp. °C	Expt.
2.21-2.29	7.10-8.14	0.126	5.0 helium	-68.0	P[1]
2.53-2.75	9.21-10.1	0.124	8.92 helium	-67.0	O[1]
2.12-2.37	14.4-15.0	0.122	15.71 helium	-68.0	N[1]
2.66-2.80	19.7-22.9	0.125	25.99 helium	-68.5	M[1]
2.38-2.72	21.1-27.9	0.066	15.61 helium	-70.7	K[1]
3.30-3.69	2.45-3.68	0.148	10.25 helium	-34.5	Q[1]
2.86-3.80	Trimer not detected	0.170	12.26 helium	+ 2.2	R[1]
3.87-4.59	9.09-12.3	0.247	8.91 nitrogen	-69.3	C[3]
3.32-4.01	0.34-0.37	0.352	9.37 nitrogen	0.0	D[2]

[a] $K_{0,1}$ refers to the reaction $NO^+ + NO \rightleftharpoons NO^+(NO)$;
$K_{1,2}$ to $NO^+(NO) + NO \rightarrow NO^+(NO)_2$.

a function of ion intensity. They were not. However, with the lamp in this configuration all the ion intensities dropped suddenly and only NO^+ could be observed. From this point on all consistent and reproducible observations in the nitric oxide system ceased. What follows is a summary of the various experiments done in an attempt to recover the complex signals.

Expt. E^2: Experiment C^2 was repeated. NO^+ was observed when the mixture was first let into the cell but it rapidly disappeared.

Expt. F^2: Experiment C^2 was repeated using helium as the diluent and NO^+, dimer and trimer were seen. They all decreased with time, the dimer and trimer going away faster than NO^+ until only NO^+ could be seen.

Expt. G^{2a}: The apparatus was let up to atmospheric pressure of helium. A lamp with a new window was installed even though the old one did not look bad. The apparatus was evacuated, Experiment F^2 was repeated, and nothing but NO^+ was seen. The stopcock to the mixing vessel was closed, the vacuum line evacuated, and pure nitric oxide let into the reaction cell up to a pressure of 9 mmHg. A small signal from the dimer may have been detected. Upon pumping out the nitric oxide and readmitting the mixture, the dimer and trimer signals were observed. $K_{0,1}$ was three times smaller and $K_{1,2}$ five times smaller than previously measured. The mixture was again isolated and the remaining gas evacuated. The next day the mixture was admitted and only NO^+ was seen. There were some signals above mass number 100. Upon exposing the cell to nitric oxide as before, the NO^+, dimer, and trimer signals were recovered.

Expt. H^2: A mixture as used in Expt. F^2 was prepared. The cell was allowed to warm to room temperature before being cooled back to -70°C.

A freshly distilled batch of nitric oxide was used in the preparation of the mixture. The mass spectrometer was set to observe the dimer signal and nitric oxide was slowly let into the reaction vessel. A signal was observed which maximized at about 0.25 mmHg. Upon pumping the nitric oxide away and letting it in again slowly, the dimer signal was observed to decay with time. The nitric oxide was pumped away and the mixture was admitted to the reaction vessel with the mass spectrometer again set to observe the dimer. When the mixture was admitted, a large signal was observed. It rapidly decayed until it was undetectable.

Expt. I^2: Setting the mass spectrometer to the dimer peak, nitric oxide was admitted and no signal was detected. The nitric oxide was pumped away and 10 to 15 microns of oxygen were admitted. Nitric oxide was slowly admitted and no dimer signal was observed. The gas was pumped away and then 10 to 15 microns of water were admitted. At -70°C the gaseous water sample condenses on the walls of the reaction vessel leaving a residual water vapor pressure of a few microns. Nitric oxide was admitted and again no dimer signal was detected. The gas was pumped away and a sample of water and 10 to 15 microns of oxygen were admitted together to the cell. Nitric oxide was let in and no dimer signal was observed.

At this time, the evidence was tending to imply that the complexes sometimes observed in the photoionization of nitric oxide were not being formed in the gas phase. The following experiments were performed with ammonia to attempt to see if the apparatus was capable of seeing complexes. At room temperature with 0.50 mmHg ammonia in the cell, photoionization of the gas produced eight signals under mass number 100. Of these NH_4^+ and NH_4^+ complexed with up to four ammonia molecules were observed.

Then a photoionization experiment, K^2, with an ammonia-helium mixture such that the spatial ion intensity in the cell would be similar to those initially apparently successful experiments with nitric oxide-helium mixtures was performed. The desired ammonia pressure using the photoionization cross sections for ammonia and nitric oxide was estimated to be 0.060 mmHg at room temperature. The helium pressure was taken to be 10 mmHg. Under these conditions NH_4^+ and complexes through the pentamer were again observed, with the tetramer being the most intense and the dimer and pentamer very weak. The measured equilibrium constant $K_{3,4}$ equal to 2.5 $(mmHg)^{-1}$ was in good agreement with Kebarle.[8]

In another experiment, L^2, an ammonia-helium mixture was prepared to give equivalent densities at 100°C but the signals were too weak to make a measurement. However, with pure ammonia at a pressure of 1 mmHg measurements could be made. A temperature run was made under these conditions. The equilibrium constant $K_{2,3}$ was measured as a function of temperature. A plot of $\ln K_{2,3}$ vs. 1/T gave a good straight line.

On the basis of the data from Expt. H^2 an estimate of the maximum value of $K_{0,1}$ was made. The dimer intensity was estimated to be the minimum detectable signal, approximately one twentieth of the NO^+ intensity. The measurement was made on a mixture of 0.25 mmHg nitric oxide with 9 mmHg helium admixed. Then $K_{0,1(Max)}$ is calculated to be 0.19 $mmHg^{-1}$ at -70°C. The fact that this number is 10 times smaller than that previously measured lends some credence to the supposition that complexes of NO^+ and nitric oxide may be formed in a surface reaction.

B. Photoionization of Ammonia

The photoionization of ammonia at room temperature produced mass resolved signals indicating that NH_4^+ had complexed with up to four molecules of ammonia. In addition signals at the following mass numbers were observed: 66, 77, 80, 83, and 125. The suggested structure for 66 was $H_2NN^+H_2(NH_3)_2$ and for 83, $H_2NN^+H_2(NH_3)_3$. The relative intensities of these and the ammonium complexes at room temperature are given in Table VI. The equilibrium constants for the (2,3) and (3,4) steps at room temperature are given in Table VII.

Table VI. Ion intensities in ammonia

	Expt. J[2] 0.50 mmHg ammonia Intensities via mass scan Resolution setting 9.2 Intensity (arb. units)	Expt. K[2] 0.050 mmHg ammonia, 10.0 mmHg helium Intensities via mass scan Resolution setting 9.2 Intensity (arb. units)
Mass		
18	120	56
35	Not detected	Not detected
52	33	66
69	100×10^1	220
86	400	21
66	225	58
77	20	Not detected
80	600	Not detected
83	190×10^1	72

Table VII. Equilibrium constants in ammonia at 294°K

Expt.	Press. (mmHg) ammonia	Press. (mmHg) helium	$K_{2,3}$ $(mmHg)^{-1}$	$K_{3,4}$ $(mmHg)^{-1}$	Resol. Setting	Method
J^2	0.57		49-62		9.2	Mass Scan
	0.50			0.72-0.88	9.2	Mass Scan
K^2	0.049	8.85	107-119		9.2	Mass Scan
	0.050	9.12		2.4 - 2.6	9.2	Mass Scan
	0.052	9.42	61-67		8.8	Fixed Point
L^2	1.00		41-48a		8.8	Fixed Point

[a] Obtained by extrapolation of $\ln K_{2,3}$ vs. 1/T plot to room temperature.

With ammonia at a pressure of about 1.0 mmHg, a temperature variation run was performed. The intensities were obtained by the fixed point method at a resolution setting of 8.8. The resolution was low enough so that this method obtained the peak intensity for a given ion. Barely detectable signals were observed at masses 18 and 35. There was a signal at mass 86 which was weak and increased slowly as the temperature was lowered. The signal at mass 59 increased at a faster rate than 86 as the temperature was lowered. As a result $K_{3,4}$ decreased from 0.237 $(mmHg)^{-1}$ at 84°C to 0.133 $(mmHg)^{-1}$ at 57.5°C. The measurements were taken by the fixed point method at the low resolution setting of 8.8 because the signals were so weak. The loss in intensity was due to the lamp window becoming colored in the center. The low resolution did not affect the reliability of $K_{2,3}$ but did affect that of $K_{3,4}$. This was due to the interference of mass 83 which was not resolved from 86. Mass 83 increased in intensity as the temperature was lowered. Under these conditions it was possible to observe the temperature dependence of $K_{2,3}$. The data from this experiment are given in Table VIII.

The $\ln K_{2,3}$ vs 1/T plot is shown in Fig. 9. From this plot an enthalpy of -12.5 to -13.5 Kcal/mole and an entropy of -22.4 to -24.8 e.u. at 298°K was derived. From Kebarle's[8] Fig. 1, we give for comparison these equilibrium constants: $K_{2,3}$ = 0.143 $(mmHg)^{-1}$ at 1.0 mmHg of ammonia and 100°C; $K_{3,4}$ = 1.32 $(mmHg)^{-1}$ at 1.0 mmHg of ammonia and 23°C. His thermodynamic data were $\Delta H_{2,3}$ = -17.8 Kcal/mole and $\Delta S_{2,3}$ = -38.0 e.u. at 298°K.

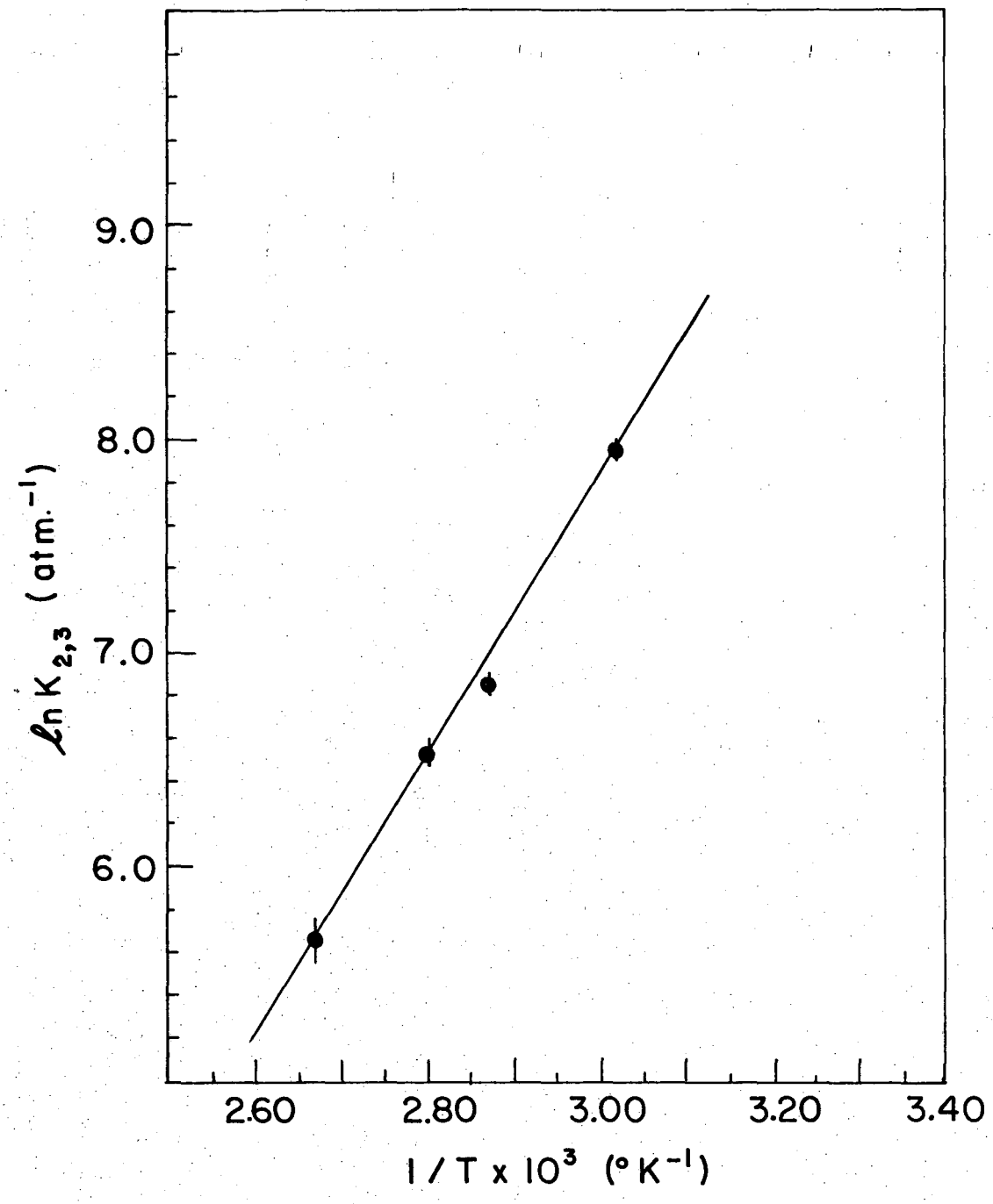

XBL688-3785

Fig. 9 Temperature dependence of $K_{2,3}$ for the reaction:

$(NH_4^+)(NH_3)_2 + NH_3 = (NH_4^+)(NH_3)_3$.

Table VIII. Equilibrium constant $K_{2,3}$ and the corresponding ion intensities as a function of temperature

Expt. L[2]				
Ammonia press. (mmHg)	1.15	1.09	1.19	1.64
Temperature (C)	57.5	74.8	84.0	100.8
Mass	Intensity (arb. units)	Intensity	Intensity	Intensity
52	16.8	35.5	22.2	6.6
69	71.9	48.2	24.1	4.1
$K_{2,3}$ $(mmHg)^{-1}$	3.72±.18	1.25±.06	0.91±.05	0.38±.02

The following conclusions could be made from these experiments. The measured equilibrium constant $K_{3,4}$ at room temperature and $K_{2,3}$ at 100°C were in reasonable agreement with that of Kebarle.[9] The effect of reducing the ammonia pressure and using helium as a third body was to increase the value of the equilibrium constants roughly by two. The plot of $\ln K_{2,3}$ vs. 1/T gives a good linear relationship and the enthalpy is in fair agreement with the values of Kebarle.[9]

C. Photoionization of Dimethylamine

The photoionization of dimethylamine produced a plethora of ions. The ion, $(CH_3)_2NH_2^+$, appeared complexed with up to five dimethylamine molecules at 20°C. These complexes were observed in the amine at a pressure of about 1 mm Hg and also at a partial pressure of 0.030 mmHg with 10.0 mmHg helium admixed. This series of ions provided the basis of a mass calibration which was used to estimate the masses of other ions detected in the photoionization of dimethylamine. The calibration also

served to determine the masses of the ions detected in the photoionization of the other two amines studied. The various ions observed in the photoionization of dimethylamine with their suggested chemical composition are listed in Table IX.

Table IX. Ionic spectrum of photoionized dimethylamine

Series I	Mass	Series I(i)	Mass
$(CH_3)_2NH^+$	45	$(CH_3)_2N^+(CH_3)_2$	87
$(CH_3)_2NH_2^+$	46		
$(CH_3)_2NH_2^+[(CH_3)_2NH]$	91	$87[(CH_3)_2NH]$	132
$46[(CH_3)_2NH]_2$	136	$87[(CH_3)_2NH]_2$	176
$46[(CH_3)_2NH]_3$	181		
etc.	226		
	271		

Series II	Mass	Series II(i)	Mass
	58		100
$58[(CH_3)_2NH]$	103	$100[(CH_3)_2NH]$	145
$58[(CH_3)_2NH]_2$	148		
etc.	193		
	235		

Series III	Mass	Series III(i)	Mass
$(CH_3)_4N^+$	74		114
$74[(CH_3)_2NH]$	119	$114[(CH_3)_2NH]$	159
$74[(CH_3)_2NH]_2$	164		
etc.	206		

1. Series I.

Under high resolution both $(CH_3)_2NH^+$ and $(CH_3)_2NH_2^+$ could be seen. The ratio of their intensities under various experimental conditions are listed in Table X.

Table X. Intensity ratio of $(CH_3)_2NH_2^+$ to $(CH_3)_2NH^+$

Expt.	Ratio 46/45	Press. (mmHg) Amine	Press. (mmHg) Helium	Temp. (C)	Lamp
Y^{2a}	2.0	1.44		21.0	Xe
Y^{2e}	3.18	2.20		144.0	Xe
R^2	1.58	0.030	16.31	21.0	Kr
S^2	1.69	0.030	4.54	20.0	Kr

The first series listed in Table VIII corresponds to dimethylamine complexing with dimethylammonium ion. From the shape of the signal at 91 under high resolution it was not possible to completely rule out there being any signal at mass 90. The maximum amount of the signal that might be due to 90 was estimated to be 25%. Comparison of the 91 signal to the 90 signal seen in the nitric oxide under the same resolution settings indicated there was no signal at 90.

As the temperature was raised the ions of Series I(i) began to interfere with those of Series I. This interference is now discussed for data taken with no helium admixed with the amine. The behavior was similar for mixtures. The intensity of the signals about five mass units lower than 91 and 136 increased as the temperature was raised. However, the masses 91 and 136 were sufficiently resolved from these ions that the

interference was not serious. The signal at mass 181 was not clearly resolved at 20°C. It was predicted to maximize at an apparent mass of 191 and observed to maximize at 189. The apparent mass number was the helipot (which controls the mass scan) setting at which the maximum signal of an ion occurred. When the temperature was raised to 53°C, the maximum signal had shifted to an apparent mass of 185. This interference of a signal about 5 mass units lower than the signal of interest was consistent with the other observations. It prevented the measurement of the intensity of mass 181 except at 20°C. Therefore the measurement of equilibrium constants was limited to $K_{0,1}$ and $K_{1,2}$ except for a tentative $K_{2,3}$ at 20°C. There were signals at the predicted positions for masses 226 and 271 but, considering the above mentioned interferences, it was impossible to determine what portions of the signals were due to these masses.

Ion intensities observed for the first series under various experimental conditions are listed in Table XI. The resolution setting in these experiments was such that ions 45 and 46 were not resolved.

Data indicating the effect of total pressure at 20°C on the measured intensities and equilibrium constants are given in Table XII. Within experimental error the equilibrium constants were independent of the total pressure of admixed helium in the range of 5 to 10 mmHg.

Data indicating the effect of the amine concentration on the measured intensities and equilibrium constants at 20°C are given in Table XIII. The total pressure of admixed helium was kept roughly constant.

Table XI. Temperature dependence of the ion intensities of Series I in dimethylamine

Mass	Expt. X^{2a} 1.45 mmHg amine Temp. 20°C Kr lamp Intensity (arb. units)	Expt. X^{2b} 1.45 mmHg amine Temp. 52.2°C Kr lamp Intensity	Expt. X^{2c} 1.69 mmHg amine Temp. 82.5°C Kr lamp Intensity
45,46 [a]	276	296	125
91	313	703	102×10^{1}
136	246×10^{2}	238×10^{2}	906×10^{1}

Mass	Expt. Y^{2a} 1.45 mmHg amine Temp. 19.8°C Xe lamp Intensity (arb. units)	Expt. Y^{2b} 1.67 mmHg amine Temp. 54.2°C Xe lamp Intensity	Expt. $Y2^{c}$ 1.69 mmHg amine Temp. 80.8°C Xe lamp Intensity
45,46 [a]	245	333	242
91	356	694	101×10^{1}
136	124×10^{2}	135×10^{2}	825×10^{1}

Mass	Expt. T^{2} 0.032 mmHg amine 8.60 mmHg helium Temp. 20.8°C Kr lamp Intensity (arb. units)	Expt. P^{2} 0.032 mmHg amine 9.54 mmHg helium Temp. 62.8°C Kr lamp Intensity	Expt. Q^{2} 0.040 mmHg amine 11.75 mmHg helium Temp. 102.8°C Kr lamp Intensity
45,46 [a]	324	558	556
91	319	254×10^{1}	511×10^{1}
136	130×10^{2}	661×10^{1}	178×10^{1}

[a] Masses 45 and 46 not resolved.

Table XII. Dependence of $K_{0,1}$ and $K_{1,2}$ for Series I on helium pressure

Mass	Expt. S^2 0.034 mmHg amine 5.20 mmHg helium Kr lamp Intensity (arb. units)	Expt. T^2 0.032 mmHg amine 8.60 mmHg helium Kr lamp Intensity	Expt. R^2 0.035 mmHg amine 19.00 mmHg helium Kr lamp Intensity
45,46 [a]	756	324	417
91	697	319	412
136	$242\ 10^2$	$130\ 10^2$	$241\ 10^2$
$K_{0,1}$ ($mmHg^{-1}$)	27-28	30-31	28-33
$K_{1,2}$ ($mmHg^{-1}$)	$830\text{-}102\times10^1$	$107\times10^1\text{-}128\times10^1$	$167\times10^1\text{-}182\times10^1$

[a] Masses 45 and 46 not resolved.

Table XIII. Dependence of $K_{0,1}$ and $K_{1,2}$ for Series I on dimethylamine concentration.

Mass	Expt. T^2 0.032 mmHg amine 8.60 mmHg helium Kr lamp Intensity (arb. units)	Expt. U^2 0.074 mmHg amine 9.40 mmHg helium Kr lamp Intensity	Expt. V^2 0.155 mmHg amine 10.6 mmHg helium Kr lamp Intensity	Expt. W^2 0.737 mmHg amine 7.82 mmHg helium Kr lamp Intensity
45,46 [a]	324	246	162	33
91	319	282	188	31
136	130×10^2	155×10^2	152×10^2	452×10^1
$K_{0,1}$ ($mmHg^{-1}$)	30-31	15-16	6.2-7.4	1.3-1.6
$K_{1,2}$ ($mmHg^{-1}$)	107×10^1-128×10^1	660-755	528-533	197-203

[a] Masses 45 and 46 not resolved.

The equilibrium constant $K_{1,2}$ is plotted as a function of amine pressure in Fig. 10. $K_{1,2}$ was observed to decrease rapidly at first and then slowly with increasing amine pressure in the experiments performed with mixtures of the amine and He. In experiments without helium the equilibrium constant was small at low amine pressures, went through a maximum at about 0.70 mmHg, and then decreased. As the amine pressure in the helium-amine experiments was raised while keeping the total pressure approximately constant, $K_{1,2}$ measured in the mixture experiments approached that measured in the experiments with no helium admixed.

This behavior indicated that equilibrium had not been achieved in the diluent experiments. The behavior in the amine without helium was more like one would expect if the reaction reached equilibrium except for the tailing down of the equilibrium constant as the pressure was increased. Also the temperature dependence will show that the measured constant $K_{1,2}$ at lower temperatures showed a curvature away from the more linear behavior of $\ln K_{1,2}$ vs $1/T$ at the higher temperatures.

To interpret this behavior we suggest two mechanisms which help explain the dependence of $\ln K_{1,2}$ on the amine pressure. After this discussion we return to the thermodynamic results.

The following mechanism is proposed to help explain the data obtained in the photoionization of dimethylamine with no helium admixed.

$AB + B \rightarrow AB_2^*$	(1)	association	$A = (CH_3)_2NH_2^+$
$AB_2^* + B \rightarrow AB_2 + B$	(2)	stabilization	$B = (CH_3)_2NH$
$AB_2^* \rightarrow AB + B$	(3)	decomposition	
$AB_2 + B \rightarrow AB_2^* + B$	(4)	excitation	
$AB_2 \rightarrow$	(5)	neutralization	
$AB_2 + B \rightarrow AB_3^*$	(6)	association	
$AB_3^* + B \rightarrow AB_3 + B$	(7)	stabilization	
$AB_3^* \rightarrow AB_2 + B$	(8)	decomposition	
$AB_3 + B \rightarrow AB_3^* + B$	(9)	excitation	

Applying the steady state approximation for AB_2^*, AB_2, and AB_3^* we get

$$(AB_2^*) = \frac{k_1(B)(AB) + k_4(B)(AB_2)}{k_2(B) + k_3}, \quad (AB_2) = \frac{k_2(AB_2^*)(B) + k_8(AB_3^*)}{k_4(B) + k_5 + k_6(B)}$$

and $$(AB_3^*) = \frac{k_6(AB_2)(B) + k_9(AB_3)(B)}{k_7(B) + k_8}$$

Substituting (AB_2^*) and (AB_3^*) into (AB_2) we get

$$(AB_2)\left[k_4(B) + k_5 + k_6(B)\right] = k_2(B)\left[\frac{k_1(B)(AB) + k_4(B)(AB_2)}{k_2(B) + k_3}\right]$$

$$+ k_8\left[\frac{k_6(AB_2)(B) + k_9(AB_3)(B)}{k_7(B) + k_8}\right] \quad . \qquad \text{(I)}$$

Rearranging we get

$$\frac{(AB_2)}{(AB)(B)}\left[k_4(B) + k_5 + k_6(B) - \frac{k_2k_4(B)^2}{k_2(B) + k_3} - \frac{k_6k_8(B)}{k_7(B) + k_8}\right] =$$

$$\left[\frac{k_1}{1 + k_3/k_2(B)}\right] + \left[\frac{k_8k_9}{k_7(B) + k_8}\right] \frac{(AB_3)}{(AB)} \quad . \qquad \text{(II)}$$

In order for the measured equilibrium constant to approach the true value as the (B) is increased, the terms involving the rate constants for the reactions (6) through (8) must be cancelled or neglected. Consider first the term

$$\left[\frac{k_8k_9}{k_7(B) + k_8}\right] \frac{(AB_3)}{(AB)} \quad .$$

We take $k_8 \gg k_7(B)$. Meisels[20] has shown that the unimolecular decay constant for $(C_6H_{12}+)^*$ is equal to or less than 10^9 sec^{-1}. $(C_6H_{12}^+)^*$ was formed by the reaction

$$C_4H_8^+ + C_2H_4 \rightarrow (C_6H_{12}^+)^*$$

If we estimate $k_7 = 10^{-10}$ cc/molec sec, $k_7(B) = 3\times10^6$ sec^{-1} with B at a pressure of 1 mmHg. Then the term above reduces to

$$\frac{k_9(AB_3)}{(AB)} \quad .$$

The rate constant k_9 is estimated to be $k_{b_1 molecule} x e^{+E/RT}$ where E is taken to be the enthalpy for the reaction

$$AB_2 + B = AB_3 \ .$$

We were not able to measure the enthalpy for the above reaction. Therefore we estimate it to be at least $1/2\Delta H_{1,2}$; $\Delta H_{1,2}$ was measured to be about -14.6 Kcal/mole. Then

$$k_9 = 10^{-10}(2\times10^{-6}) = 2\times10^{-16} \text{ cc/molec sec}$$

The ratio, $(AB_3)/(AB)$, was approximately 10 at 1.45 mmHg of dimethylamine. Then the expression

$$k_9(AB_3)/(AB) = 2\times10^{-15} \text{ cc/molec sec}$$

We now consider the term

$$\frac{k_1}{1 + \frac{k_3}{k_2(B)}}$$

and we assume $k_3 \gg k_2(B)$ for the same reason we assumed $k_8 \gg k_7(B)$. Then it reduces to

$$\frac{k_1 k_2(B)}{k_3} \quad .$$

We estimate $k_1 = k_2 = 10^{-10}$cc/molec sec and $k_3 = 10^9$ sec^{-1}; $k_2(B) = 3\times10^6$ sec^{-1} with B at 1.0 mmHg pressure. Then the term

$$\frac{k_1 k_2(B)}{k_3} = 3\times10^{-13} \text{ cc/molec sec.}$$

Thus we see we can neglect the term

$$\frac{k_8 k_9 \quad (AB_3)}{k_7(B) + k_8 \quad (AB)}$$

in comparison to

$$\frac{k_1 k_2(B)}{k_3} \quad .$$

Also the terms

$$k_6(B) - \frac{k_6 k_8(B)}{k_7(B) + k_8}$$

cancel under the assumption $k_8 \gg k_7(B)$.

Equation (II) then becomes

$$\frac{(AB_2)}{(AB)(B)} = \frac{k_1 k_2(B)}{k_3\left[k_4(B) - \frac{k_2 k_4(B)^2}{k_2(B)+k_3} + k_5\right]} \qquad \text{(III)}$$

With the assumption that $k_3 \gg k_2(B)$, the terms

$$k_4(B) - \frac{k_2 k_4(B)^2}{k_2(B)+k_3} = k_4(B)\left[1 - \frac{k_2(B)}{k_2(B) + k_3}\right]$$

reduce to $k_4(B)$. Equation (III) then becomes

$$\frac{(AB_2)}{(AB)(B)} = \frac{k_1 k_2(B)}{k_3[k_4(B)+k_5]} \qquad \text{(IV)}$$

Equation (IV) predicts that the measured equilibrium constant should be small at low (B) and should increase as the (B) is raised. This is seen to be the case in Fig. 10 with the exception that the measured equilibrium constant goes through a maxium and then tails down as the amine pressure is further increased.

If the preceding assumptions are valid, equilibrium should be achieved when $k_4(B) \gg k_5$. We estimate k_5 to be $k_n(N^-) = 1.0\ sec^{-1}$ where k_n, the neutralization rate constant, is taken to be 10^{-7} cc/molec sec and (N^-), the concentration of negative particles, is taken to be 10^7 ions/cc.

If we require that $k_4(B) > 10\ sec^{-1}$ with $(B) = 3\times10^{16}$ mole/cc, k_4 is at least 3×10^{-17} cc/mole sec. From Fig. 10 the true value of $K_{1,2}$ is estimated to be 150 $mmHg^{-1}$. Use of the equation

$$K_{1,2} = \frac{k_1 k_2}{k_3 k_4} (3\times10^{16}\ mmHg^{-1})$$

permits a derivation of k_3 equal to $5\times10^{10}\ sec^{-1}$ if we take $k_1 = k_2 = 10^{-10}$ cc/mole sec and $k_4 = 3\times10^{-17}$ cc/molec sec.

To interpret the behavior in the mixture experiments the following mechanism is proposed. A main assumption is that $(CH_3)_2NH_2^+[(CH_3)_2NH]$ is lost at a faster rate than $(CH_3)_2NH_2^+\ [(CH_3)_2NH]_2$. Also we observe that $K_{0,1}$ of Series I in dimethylamine shows the wrong temperature dependence; that is, it gets larger as the temperature is increased. We conclude that the (0,1) step is not at equilibrium. If equilibrium is not attained, one expects that the rate of re-excitation of the stabilized complex, $(CH_3)_2NH_2^+[(CH_3)_2NH]$, is not fast enough. Therefore in the following mechanism we neglect the collisional excitation of this ion.

$A + B \rightarrow AB^*$	(a) association	$A = (CH_3)_2NH_2^+$
$AB^* \rightarrow A + B$	(b) decomposition	$B = (CH_3)_2NH$
$AB^* + He \rightarrow AB + He$	(c) stabilization	
$AB \rightarrow$	(x) loss	
$AB + B \rightarrow AB_2^*$	(d) association	
$AB_2^* + He \rightarrow AB_2 + He$	(e) stabilization	
$AB_2^* \rightarrow AB + B$	(f) decomposition	
$AB_2 + He \rightarrow AB_2^* + He$	(g) excitation	

Applying the steady state approximation to AB^*, AB, and AB_2^*, we get

$$(AB^*) = \frac{k_a(A)(B)}{k_b + k_c(He)}, \quad (AB) = \frac{k_f(AB_2^*) + k_c(He)(AB^*)}{k_x + k_d(B)},$$

and

$$(AB_2^*) = \frac{k_d(B)(AB) + k_g(AB_2)(He)}{k_e(He) + k_f}.$$

If we substitute (AB_2^*) and (AB^*) into the expression for (AB), it follows that

$$(AB) = \left[\frac{k_f[k_d(B)(AB) + k_g(AB_2)(He)}{k_e(He) + k_f} + \frac{k_c(He)k_a(A)(B)}{k_b + k_c(He)}\right] \Big/ [k_x + k_d(B)]. \tag{V}$$

When we rearrange Eq. (V), we get

$$K_{1,2} = \frac{(AB_2)}{(AB)(B)} = \frac{k_d k_e}{k_f k_g} + \left[\frac{k_e(He) + k_f}{k_f k_g}\right]\left[\frac{k_x}{(B)(He)} - \frac{k_c k_a(A)}{(AB)[\ k_c(He)+k_b\ ]}\right]. \tag{VI}$$

We note that $K_{1,2}$ will be independent of (B) if $k_x = k_i(B)$ where k_i is an ion-molecule reaction rate constant. From Fig. 11 we see that $K_{1,2}$ is inversely proportional to (B). Thus we conclude the loss process is not due to an ion-molecule reaction.

We now suppose that the loss process is deionization. Then $k_x = k_n(A^-)$ where k_n is the neutralization rate constant and (A^-) is the concentration of recombining negative particles. With $k_n = 10^{-7}$ cc/mole sec and $(A^-) = 10^7$ ions/cc, $k_x = 1.0\ sec^{-1}$.

We consider the terms

$$\frac{k_x}{(B)(He)} - \frac{k_c k_a (A)}{(AB)\,[k_c(He) + k_b]} \quad . \qquad \text{(VII)}$$

Experimentally we measure (A)/(AB) approximately equal to 1.0. If $k_c(He) \gg k_b$, the expression VII reduces to

$$\frac{[h_x/(B)] - k_a}{(He)} \quad .$$

With B at 0.10 mmHg we estimate $k_x/(B) = 1.0\ sec^{-1}\ 3\times10^{15}$ molec/cc = 3×10^{-16} cc/molec sec. If we take k_a to be the order of a bimolecular collisional rate constant, 10^{-10} cc/molec sec, we see that k_x would have to be a factor of 10^6 larger to compensate for k_a.

If we now assume $k_b \gg k_c(He)$, the terms of Expression (VII) become

$$\frac{k_x}{(B)(He)} - \frac{k_c k_a}{k_b} \quad .$$

We estimate

$$\frac{k_x}{(B)(He)} = \frac{1.0\ sec^{-1}}{3\times10^{15}\ 3\times10^{17} molec^2/cc^2} = 10^{-33}\ cc^2/molec^2\ sec$$

with helium at 10 mmHg. We estimate $k_a = 10^{-10}$ cc/mole possibly as low as 10^{-12} cc/molec sec. In keeping with our other assumptions about unimolecular rate constants, we estimate $k_b = 10^9\ sec^{-1}$. Then

$$\frac{k_c k_a}{k_b} = 10^{-31}\ cc^2/molec^2\ sec \quad .$$

We still have the situation that the correction term to the true equilibrium constant is negative, but the two terms are much closer than in the other case.

Now we calculate the correction term,

$$\left[\frac{k_e(He) + k_f}{k_f k_y}\right]\left[\frac{k_x}{(B)(He)} - \frac{k_c k_a}{k_b}\right] 3\times10^{16}\ \text{mmHg}^{-1}$$

We have previously derived a value of $k_f = 5\ 10^{10}\ \text{sec}^{-1}$ ($k_f = k_3$) and therefore $k_f \gg k_e$ (He). For the reaction

$$AB_2 + B \rightarrow AB_2^*$$

we have indicated that the rate constant is at least equal to 3×10^{-17} cc/molec sec. For the reaction

$$AB_2^* + He \xrightarrow{k_4} AB_2$$

we estimate $k_g = k_{bimolec} x e^{+E/kT}$. We take E to be the experimentally measured enthalpy for the reaction

$$AB + B = AB_2 \quad .$$

Then $k_g = 10^{-10}\times10^{-9} = 10^{-19}$ cc/molec sec. We now substitute our estimates of $k_x/(B)(He)$ and $k_c k_a/k_b$, respectively into the correction term to see which is closer to the observed effect. The correction term is

$$\frac{(10^{-33}\ \text{or}\ 10^{-31})\ 3\times10^{16}\ \text{mmHg}^{-1}}{10^{-19}} = (3\times10^{2}\ \text{or}\ 3\times10^{4})\ \text{mmHg}^{-1} \quad .$$

We are doing this calculation for B at a pressure of 0.10 mmHg. At this pressure we measure $K_{1,2}$ to be 600 mmHg^{-1}. The term $k_x/(B)(He)$ is then the correct order of magnitude. Also we observe that the total ion concentration is approximately the same in 0.10 mmHg of dimethylamine with 10.0 mmHg helium admixed as in the amine at 1.4 mmHg. Therefore we expect k_x to be similar in both situations. Thus we say that k_b was

under estimated and require it to be of the order of 10^{11} sec^{-1}. The correction factor now could be in the range observed if k_x were 5 sec^{-1}.

In conclusion we can say that the mechanisms predict the right qualitative behavior which was observed. One can combine the two mechanisms with the experimental results to obtain values for the constants k_3 and k_4 which give some consistency to both types of experiments.

The equilibrium constants for the addition of dimethylamine to dimethylammonium ion are listed in Table XIV as a function of temperature. Plots of $\ln K_{1,2}$ vs 1/T are given in Figs. 12-14. The temperature dependence of the equilibrium constant $K_{1,2}$ in the amine with no helium admixed was not very satisfactory. The slope approaches that of the mixture measurements as the temperature increases. The absolute values of the equilibrium constants are different in the mixture and the amine with no He admixed experiments. It should be noted that at the higher temperatures the signals which were about five mass units lower than the signals of interest were equal to or larger than those of Series I.

The $\ln K_{1,2}$ vs 1/T plot for data taken in the amine with no helium admixed showed considerable curvature at the lower temperatures. Therefore the lines from which the enthalpies were estimated were drawn to fit the data at the higher temperatures. Values of the enthalpy and entropy derived from these plots are given in Table XV.

Table XIV. Temperature dependence of the equilibrium constants $K_{0,1}$ and $K_{1,2}$ for Series I in dimethylamine

Expt.	Pressure (mmHg) amine	Pressure (mmHg) helium	Temp. (C)	$K_{0,1}(mmHg)^{-1}$	$K_{1,2}(mmHg)^{-1}$	$K_{3,4}(mmHg)^{-1}$	Lamp
X^{2a}	1.45		20.0	0.799-0.710	54.3-40.0	0.103	Kr
$X2^{b}$	1.45		52.2	1.64-1.48	23.3-20.0		Kr
X^{2c}	1.69		82.5	4.82-4.44	8.92-8.47		Kr
X^{2d}	1.77		101.5	12.7-11.0	1.94-2.29		Kr
X^{2e}	2.10		131.2	14.9-16.4	0.394-0.412		Kr
T^{2}	0.032	8.60	20.8	30-32	1278-1067		Kr
P^{2}	0.032	9.54	62.8	142-128	81.5-76.5		Kr
Q^{2}	0.040	11.70	102.8	224-273	8.69-8.31		Kr
Y^{2ar}	1.45		19.8	1.07-1.00	24.3-20.0		Xe
Y^{2b}	1.67		54.2	1.24-1.18	11.6-12.0		Xe
Y^{2c}	1.69		80.8	2.47-2.70	4.80-4.91		Xe
Y^{2d}	1.91		112.2	4.88-4.10	1.06-1.03		Xe
Y^{2e}	2.20		145.0	4.90-	0.166		Xe

Table XV. Enthalpy and entropy for the (1,2) step for Series I in dimethylamine

Expt.	$\Delta H_{1,2}$ (Kcal/mole)	$\Delta S_{1,2}(294)$ e.u.
Amine Kr Lamp	-11.9 to -13.9	-17.3 to -22.3
Amine Xe Lamp	-13.6 to -15.6	-22.5 to -27.6
Mixture Kr Lamp	-13.1 to -13.8	-17.5 to -19.3

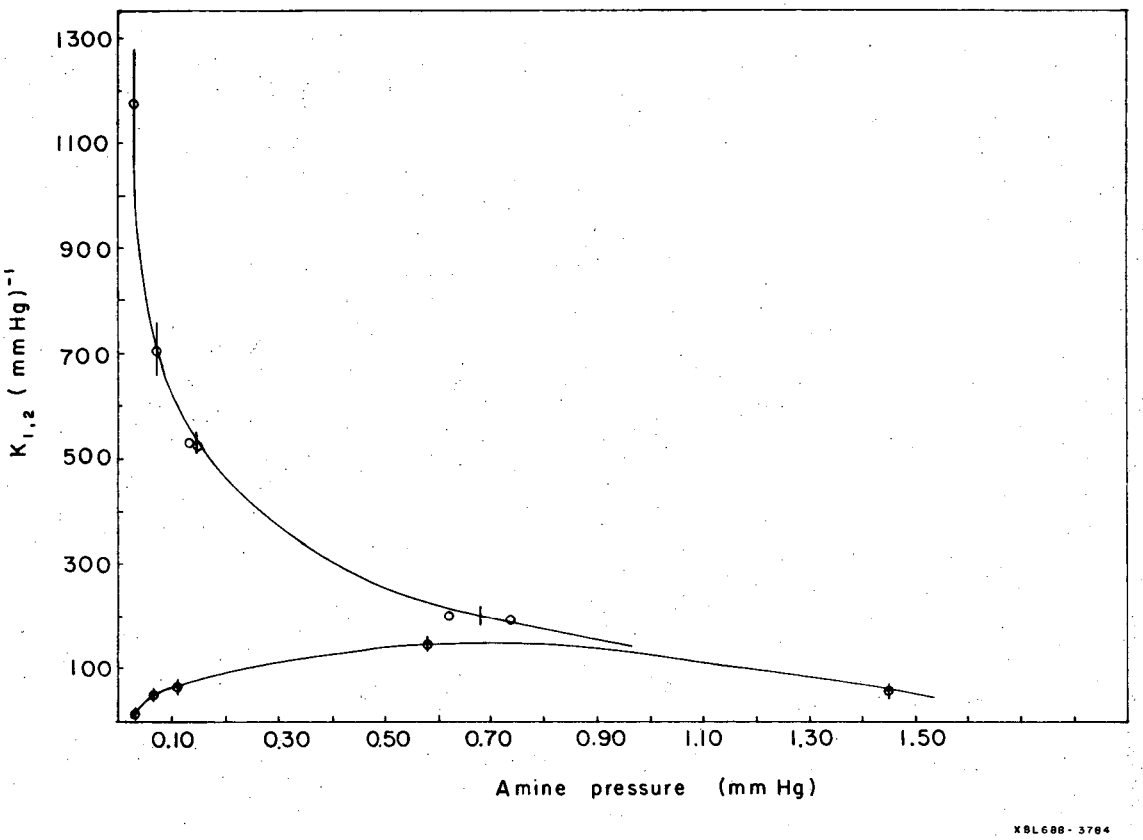

Fig. 10 Dependence of $K_{1,2}$ on dimethylamine pressure for Series I. (ϕ) mixture of amine and helium with the total pressure about 10.0 mmHg, (ϕ) amine with no helium admixed.

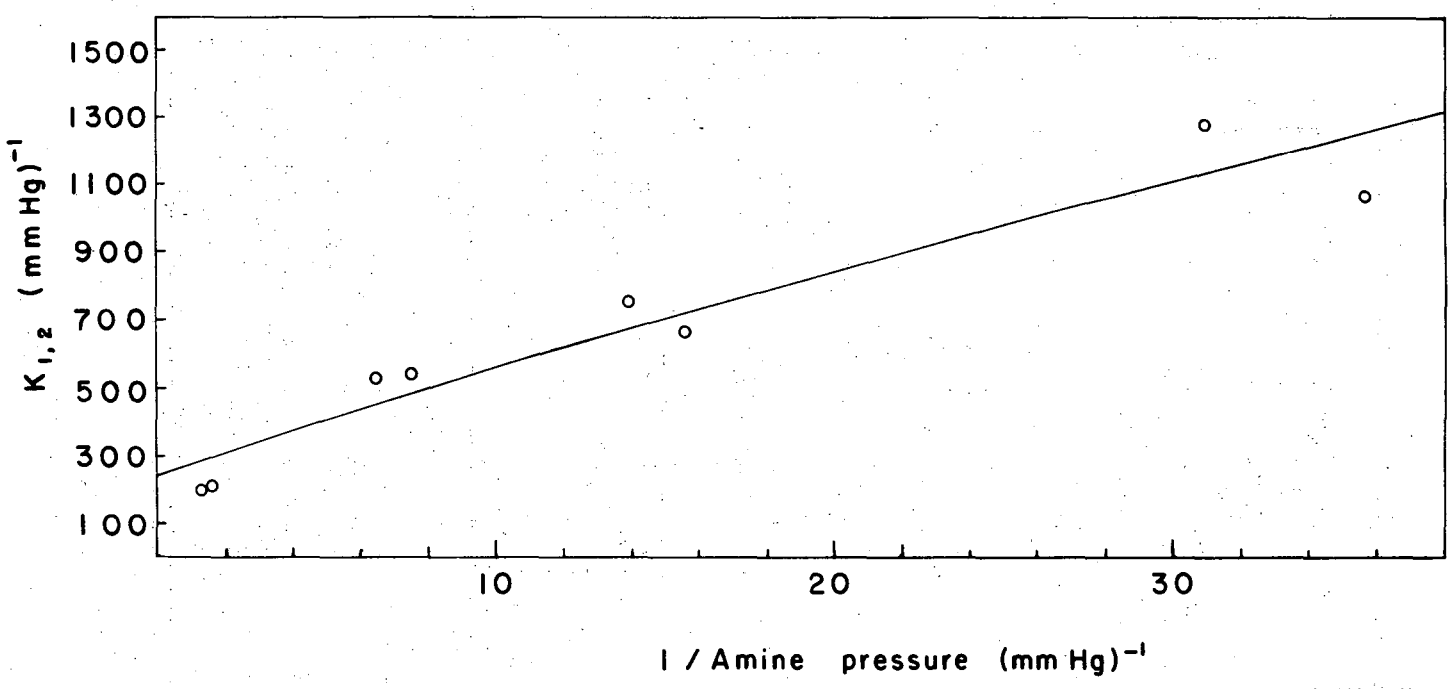

Fig. 11 Plot of $K_{1,2}$ vs. 1/(pressure of dimethylamine) for Series I with helium added to make the total pressure about 10.0 mmHg.

2. Series II

The chemical identity of mass 58 has not been determined. When it was compared to the 59,60 signal, trimethylamine and trimethylammonium ion, detected in the photoionization of trimethylamine, it appeared 1 mass unit lower. At 20°C the signals at masses 103 and 148 were covered by the two signals of Series II(i), 100 and 145. When the temperature was raised to 83°C, the ions 103 and 148 had become predominant.

The equilibrium constant for the addition of dimethylamine to the mass 58 ion showed the wrong temperature dependence at the lower temperatures. The second step showed the correct temperature dependence but the linearity of $\ln K_{1,2}$ was not very good. The data are given in Table XVI.

Table XVI. Equilibrium constants $K_{0,1}$ and $K_{1,2}$ for Series II in dimethylamine and the corresponding ion intensities as a function of temperature.

Mass	Expt. Y^{2c} 1.72 mmHg amine Temp. 83.5°C Xe lamp Intensity(arb. units)	Expt. Y^{2d} 1.92 mmHg amine Temp. 116° C Xe lamp Intensity	Expt. Y^{2e} 2.20 mmHg amine Temp. 144°C Xe lamp Intensity
58	42	66	285
103	480	183×10^{1}	482×10^{1}
148	608×10^{1}	932×10^{1}	750×10^{1}
$K_{0,1}(\text{mmHg})^{-1}$	6.7±.3	14.4±.7	7.68±.4
$K_{1,2}(\text{mmHg})^{-1}$	7.38±.3	2.65±.1	0.709±.03

3. Series III

The ion observed at mass 74 was believed due to tetramethylammonium ion. It coincided with a signal attributed to tetramethylammonium ion seen in the photoionization of trimethylamine. The ions at masses 119 and 164 were attributed to mass 74 complexing respectively with one and two molecules of dimethylamine. Masses 119 and 164 were interfered with by the two ions, 114 and 159, of Series III(i). At 117.8°C mass 114 was as intense as 119; at 83.5°C mass 159 was as intense as 164. There were signals where 206 and 249 were expected to come but the contribution of these signals to the masses 206 and 249 could not be determined. The equilibrium constant for the addition of dimethylamine to the mass 74 ion showed the wrong temperature dependence at the lower temperatures. The second step showed the right temperature dependence and the linearity of $\ln K_{1,2}$ vs. 1/T was good. The data are given in Table XVI. A plot of $\ln K_{1,2}$ vs. 1/T can be seen in Fig. 15. From this plot an enthalpy of -12.2 to -14.1 Kcal/mole and an entropy of -20.6 to -26.2 e.u. at 294°K were derived.

Table XVII. Equilibrium constants $K_{0,1}$ and $K_{1,2}$ for Series III in dimethylamine and the corresponding ion intensities as a function of temperature.

Mass	Expt. Y^{2a} 1.46 mmHg amine Temp. 20.5°C Xe lamp Intensity (arb. units)	Expt. Y^{2b} 1.68 mmHg amine Temp. 57°C Xe lamp Intensity	Expt. Y^{2c} 1.72 mmHg amine Temp. 83.5°C Xe lamp Intensity	Expt. Y^{2d} 1.92 mmHg amine Temp. 117.5°C Xe lamp Intensity
74	13	21	40	125
119	35	494	146×10^{1}	122×10^{1}
164	255×10^{1}	445×10^{1}	283×10^{1}	
$K_{0,1}$ ($mmHg^{-1}$)	1.8±.1	14±.7	21±1	9.3±.4
$K_{1,2}$ ($mmHg^{-1}$)	50±3	5.36±.3	1.13±.06	

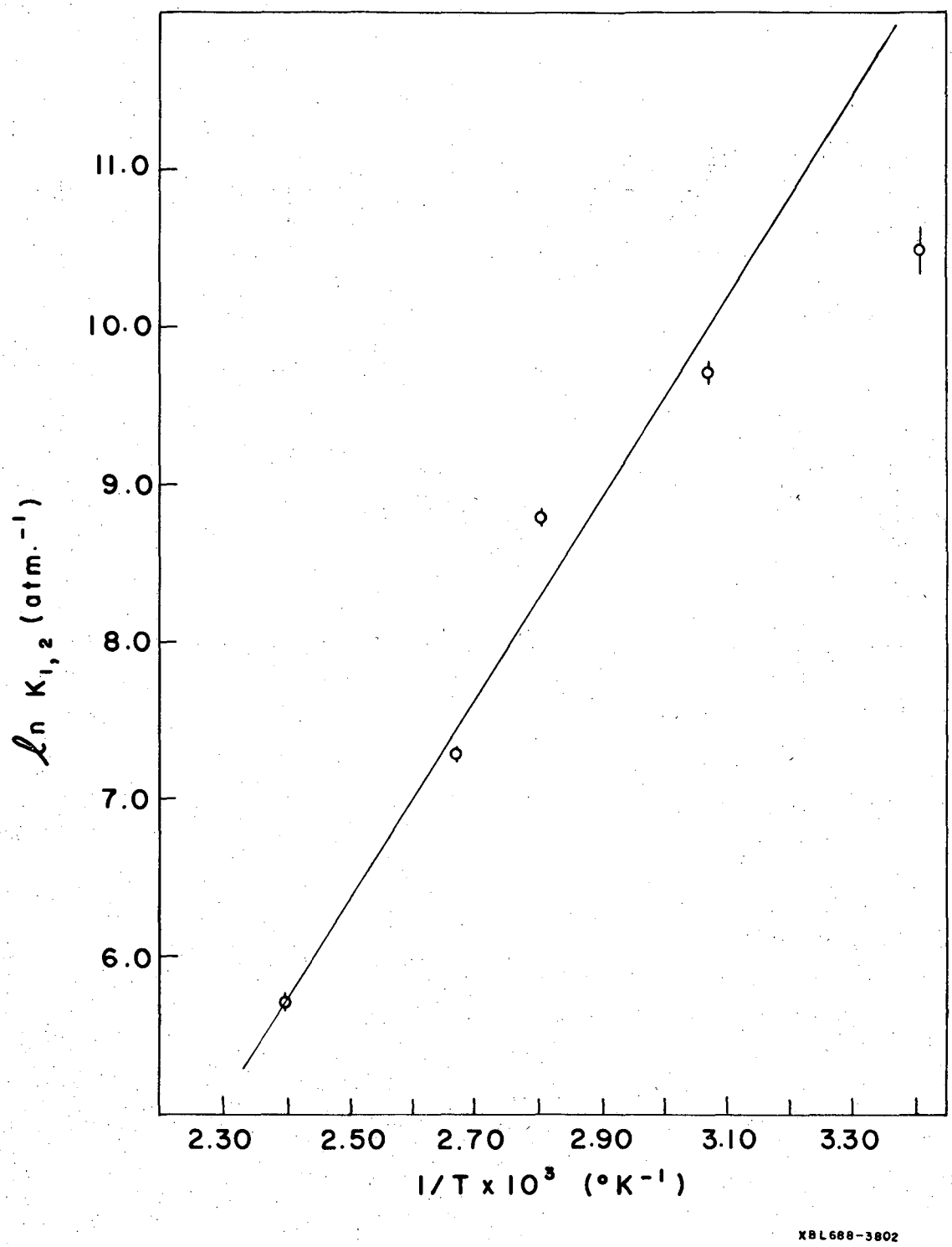

Fig. 12 Temperature dependence of $K_{1,2}$ for Series I in dimethylamine with a krypton lamp.

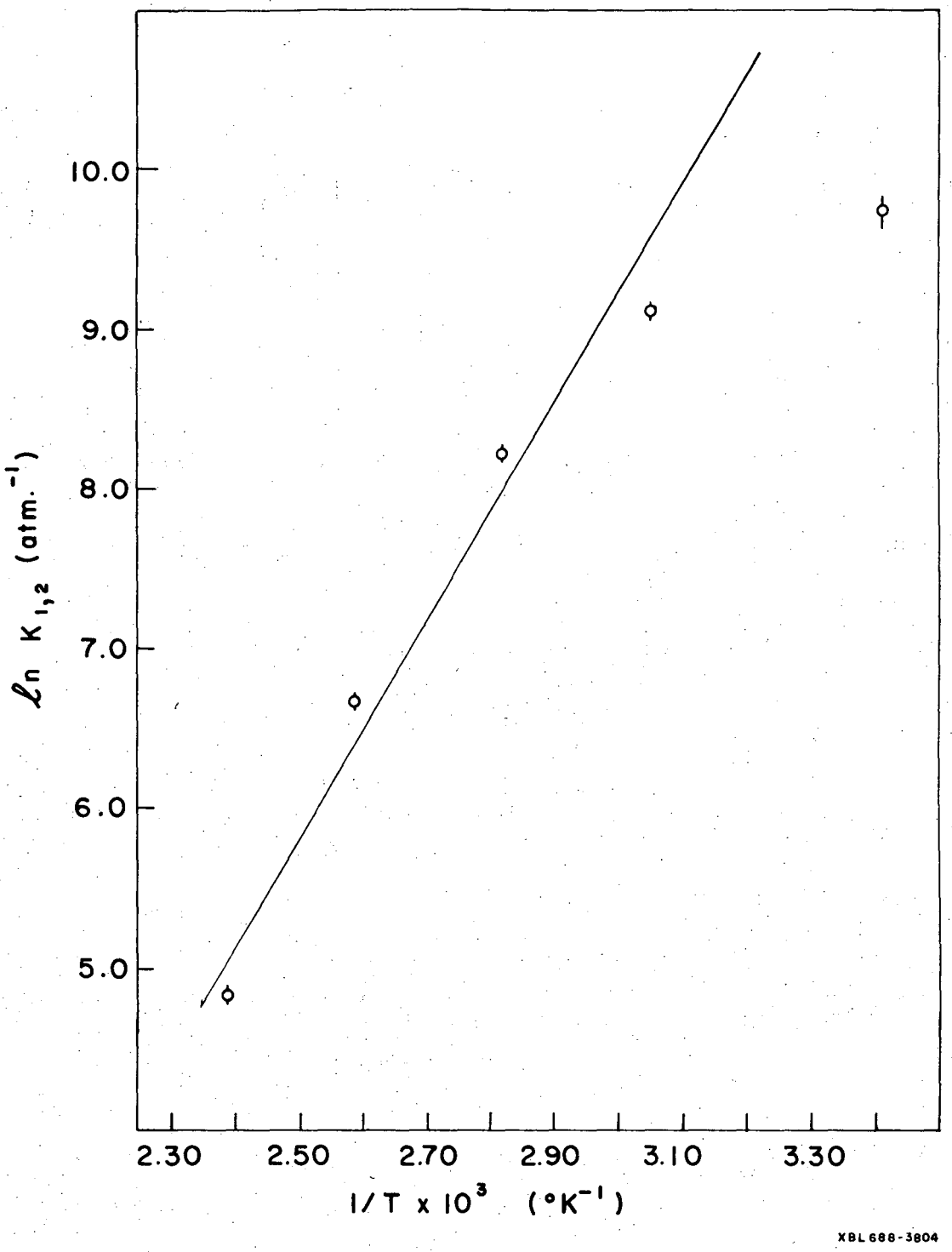

Fig. 13 Temperature dependence of $K_{1,2}$ for Series I in dimethylamine with a xenon lamp.

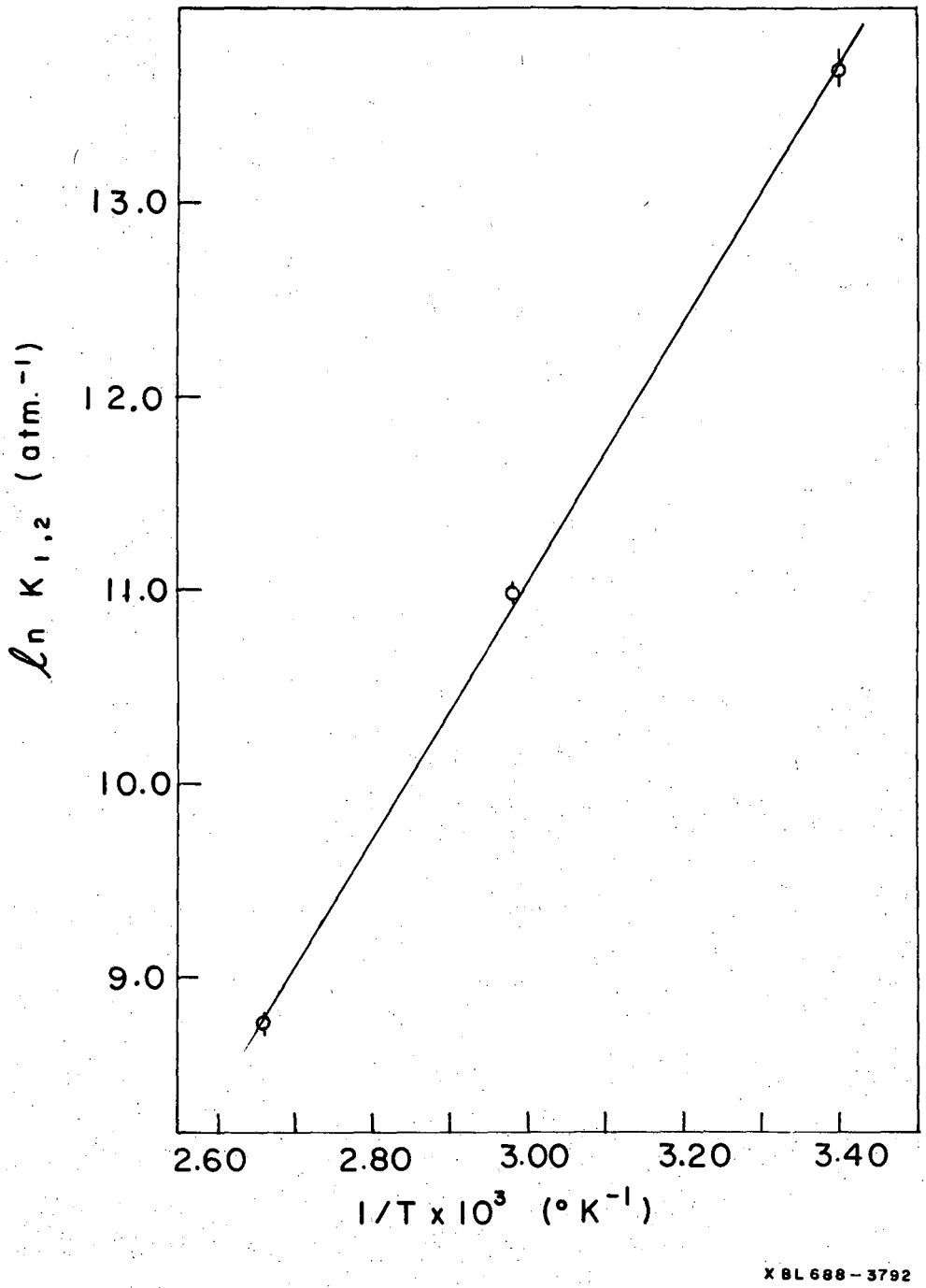

Fig. 14 Temperature dependence of $K_{1,2}$ for Series I in mixtures of dimethylamine and helium with a krypton lamp.

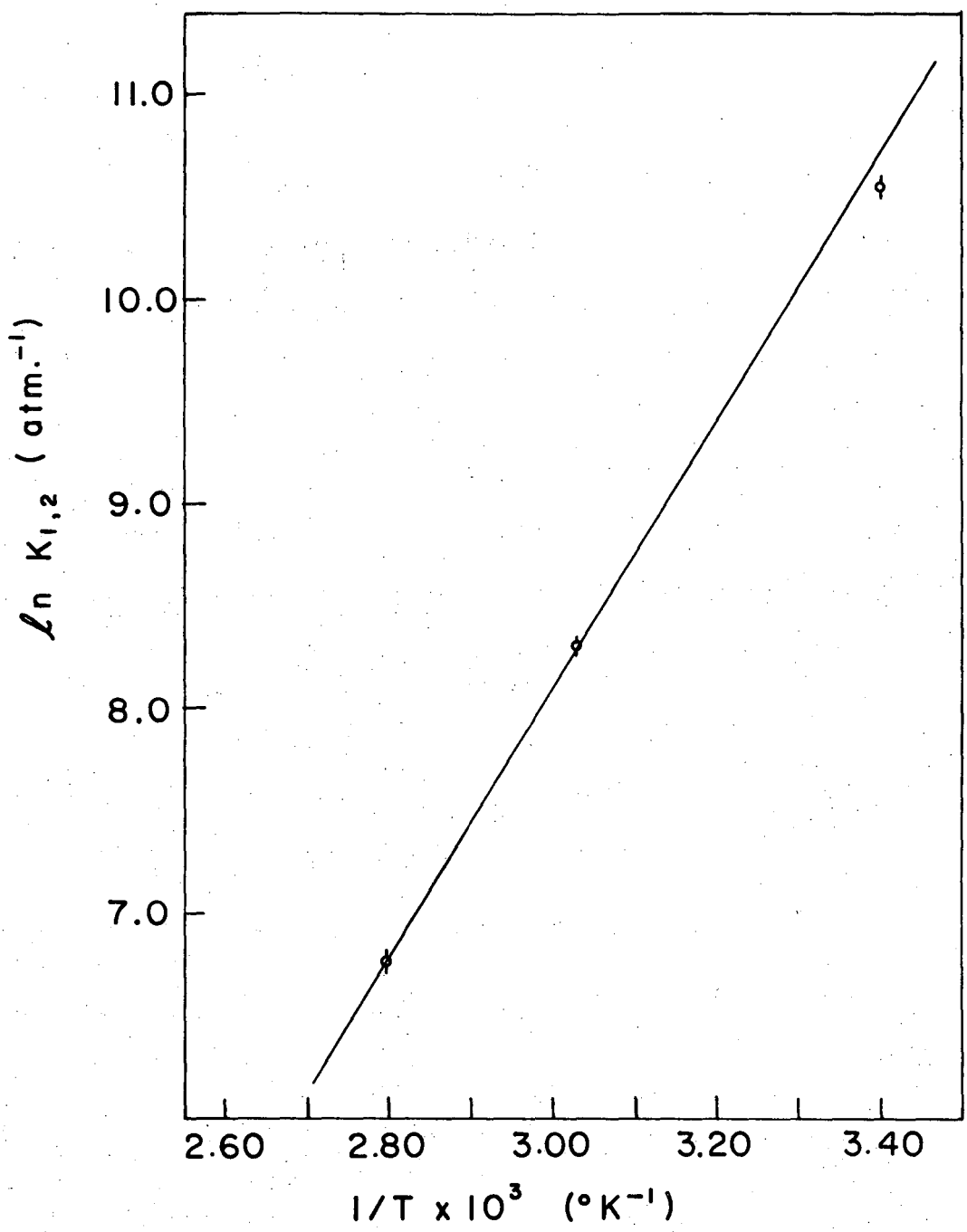

XBL688-3790

Fig. 15 Temperature dependence of $K_{1,2}$ for Series III in dimethylamine.

D. Photoionization of Trimethylamine

The photoionization of trimethylamine produced a large number of signals. The ion, $(CH_3)_3NH^+$, was seen complexed with up to 3 molecules of trimethylamine. Using the mass calibration prepared in the dimethylamine study, these ions appeared at mass numbers 59.5, 119, 177, and 233. The complexes were detected in the amine at a pressure of 1 mmHg and also at a partial pressure of 0.030 mmHg with 10.0 mmHg helium admixed. The various ions observed in the photoionization of trimethylamine with their suggested chemical composition are listed in Table XVIII. Since the ions in Series III and IV were investigated in only one experiment, no additional data will be tabulated for them.

Table XVIII Ionic spectrum of photoionized trimethylamine

Series I	Mass	Series I(i)	Mass
$(CH_3)_3N^+$	59		117
$(CH_3)_3NH^+$	60	$117[(CH_3)_3N]$	175
$(CH_3)_3NH^+[(CH_3)_3N]$	119	$117[(CH_3)N]_2$	234
etc.	178		
	237		

Series II	Mass	Series II(i)	Mass	Series III	Mass
$(CH_3)_4N^+$	74		132		
$(CH_3)_4N^+[(CH_3)_3N]$	133	$132[(CH_3)N]$	190	$(CH_3)_2NN^+(CH_3)_2$	87
etc.	192			$87[(CH_3)_3N]$	144
					147

Series IV	Mass
	101
	103
	108
$101[(CH_3)_3N]$	160

1. Series I

Under high resolution $(CH_3)_3N^+$ and $(CH_3)_3NH^+$ were detected. The ratio of their intensities under the various experimental conditions are listed in Table XIX.

Table XIX. Intensity ratio of $(CH_3)_3NH^+$ to $(CH_3)N^+$

Expt.	Ratio 60/59	Press. (mmHg) amine	Press. (mmHg) helium	Temp. (C)
A^{3a}	1.45	1.21		20.0
A^{3d}	1.69	1.91		118.5
B^3	0.79	0.024	10.50	20.0
E^3	1.75	0.028	9.50	118.5

The first series listed in Table XVIII was attributed to trimethylamine complexing with trimethylammonium ion. The mass spectrometer could not determine whether $(CH_3)_3N^+[(CH_3)_3N]$ contributed to the signal detected at mass 119. The mass spectrometric observations made in methylamine and dimethylamine indicated that the ammoniated amine ion was responsible for the first ion-amine complex. Also the equilibrium constant data obtained in dimethylamine and trimethylamine substantiated this suggestion. The equilibrium constant information is discussed in Section VII.

As the temperature was raised, the ions of Series I(i) began to interfere with those of Series I. The interferences were serious because the ions of Series I(i) were only two mass units lower than the ones with which they interfered. The following discussion refers

to observations made in the amine with no helium admixed. The behavior was similar in the mixture experiments. At 81°C the interference had become significant. Here the relative intensities were the following: 117/119 = 0.30, 175/177 = 0.44, and 234/236 = 0.80. The nonlinear behavior of $\ln K_{2,3}$ vs 1/T and $\ln K_{1,2}$ to a lesser degree was probably due to these interferences at higher temperatures. Ion intensities of Series I as a function of temperature are listed in Table XX. The resolution in these experiments was such that 59 and 60 were not resolved. All the data refer to photoionization of trimethylamine with a Xe lamp.

Table XX. Temperature dependence of ion intensities for Series I in trimethylamine

Mass	Expt. A[3ar] 1.21 mmHg amine Temp. 21°C Intensity (arb. units)	Expt. A[3b] 1.44 mm Hg amine Temp. 54.6°C Intensity
59,60[a]	139×10^{1}	109×10^{1}
119	302×10^{2}	420×10^{2}
178	241×10^{2}	180×10^{1}
237	700×10^{1}	251×10^{1}

Mass	Expt. B[3] 0.028 mmHg amine 12.03 mmHg helium Temp. 19.8°C Intensity (arb. units)	Expt. C[3] 0.032 mmHg amine 10.08 mmHg helium Temp. 54.8°C Intensity
59,60[a]	309	633
119	322×10^{1}	867×10^{1}
178	900	778
237	96	73

[a] Masses 59 and 60 not resolved

The equilibrium constants for the addition of trimethylamine to trimethylammonium ion are listed in Table XXI as a function of temperature. Plots of lnK vs. 1/T are shown in Figs. 16 and 17. From these plots and Table XXI one can see that the temperature dependence of the equilibrium constants was similar in the amine and in the amine with helium admixed. Values of the enthalpy and entropy derived from these plots are given in Table XXII.

2. Series II.

The second series of signals in Table XXIII was attributed to tetramethylammonium ion complexing with trimethylamine. The signals at masses 133 and 192 were interfered with by ions at masses 131 and 190 respectively. At 82.8°C the ratio of mass 131 to 133 was 0.6 and the ratio of 190 to 192 was 0.7. The data for this series are given in Table XXIII. A plot of $\ln K_{1,2}$ vs. 1/T is given in Fig. 18. From this plot an enthalpy of -5.23 to -6.06 Kcal/mole and an entropy of -3.6 to -6.2 e.u. at 294°K were derived.

Table XXI. Temperature dependence of the equilibrium constants $K_{0,1}$, $K_{1,2}$ and $K_{2,3}$ for Series I in trimethylamine

Expt.	Pressure (mmHg) amine	Pressure (mmHg) helium	Temp. (C)	$K_{0,1}$ $(mmHg)^{-1}$	$K_{1,2}$ $(mmHg)^{-1}$	$K_{2,3}$ $(mmHg)^{-1}$
A^{3ar}	1.21		21.0	23.7-20.2	0.662-0.673	0.241-0.235
A^{3b}	1.44		54.6	26.8-25.0	0.298-0.349	0.0965-0.0924
A^{3c}	1.68		81.0	24.2-24.1	0.138-0.137	0.0645-0.0665
A^{3d}	1.90		118.5	18.2-21.2	0.0347-0.0403	0.0567-0.0586
B^3	0.027	11.68	19.8	380.-418.	13.6-16.5	3.89-4.68
C^3	0.031	10.62	54.8	422.-515	2.80-3.61	2.48-3.22
D^3	0.032	10.85	85.8	353.-413.	1.21-1.36	(a)
E^3	0.034	11.24	118.5	269.-350.	0.507-0.597	(a)

[a] The signal at mass 237 was weak and interfered with by other signals. Therefore, $K_{2,3}$ could not be measured.

Table XXII. Enthalpy and entropy of the (1,2) and (2,3) steps for Series I in trimethylamine

Expt.	$\Delta H_{1,2}$ (Kcal/mole)	$\Delta S_{1,2(294K)}$ (e.u.)	$\Delta H_{2,3}$ (Kcal/mole	$\Delta S_{2,3(294K)}$ (e.u.)
Amine	-7.95 to -9.50	-13.3 to -17.7	-4.07 to -4.83	-3.7 to -6.0
Mixture	-7.19 to -8.03	-6.16 to -8.65		

Table XXIII. Temperature dependence of the equilibrium constants $K_{0,1}$ and $K_{1,2}$ for Series II in trimethylamine and the corresponding ion intensities.

Mass	Expt. A[3a] 1.26 mmHg amine Temp. 19.8°C Intensity (arb. units)	Expt. A[3b] 1.44 mmHg amine Temp. 55.2°C Intensity	Expt. A[3c] 1.67 mmHg amine Temp. 82.8°C Intensity
74	17	35	73
133	117×10^{1}	458×10^{1}	393×10^{1}
192	267×10^{1}	400×10^{1}	865
$K_{0,1}$ ($mmHg^{-1}$)	54±3	91±4	28±2
$K_{1,2}$ ($mmHg^{-1}$)	1.82±.09	0.606±.03	0.115±.006

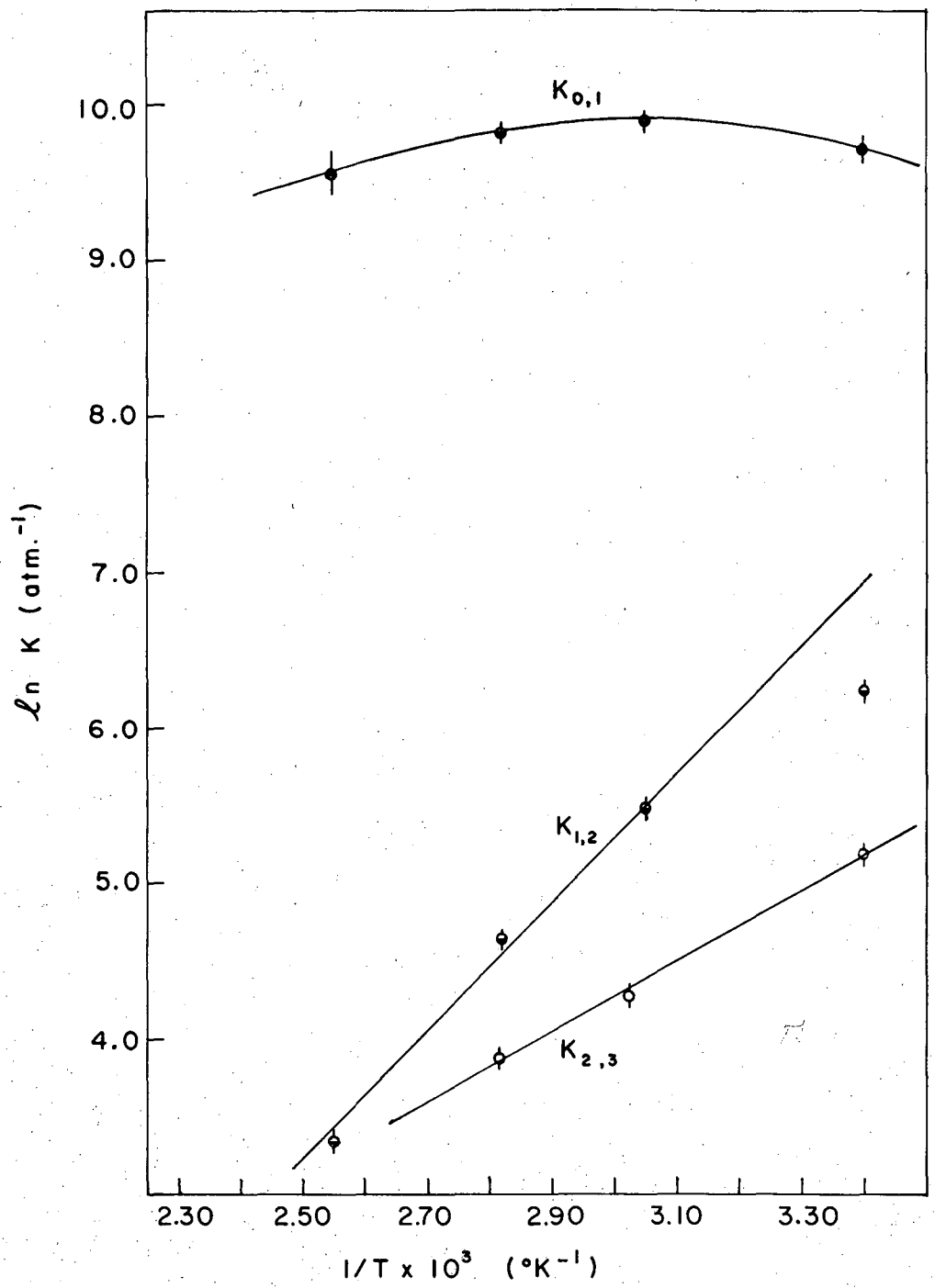

X BL688-3791

Fig. 16 Temperature dependence of $K_{0,1}$, $K_{1,2}$, and $K_{2,3}$ for Series I in trimethylamine.

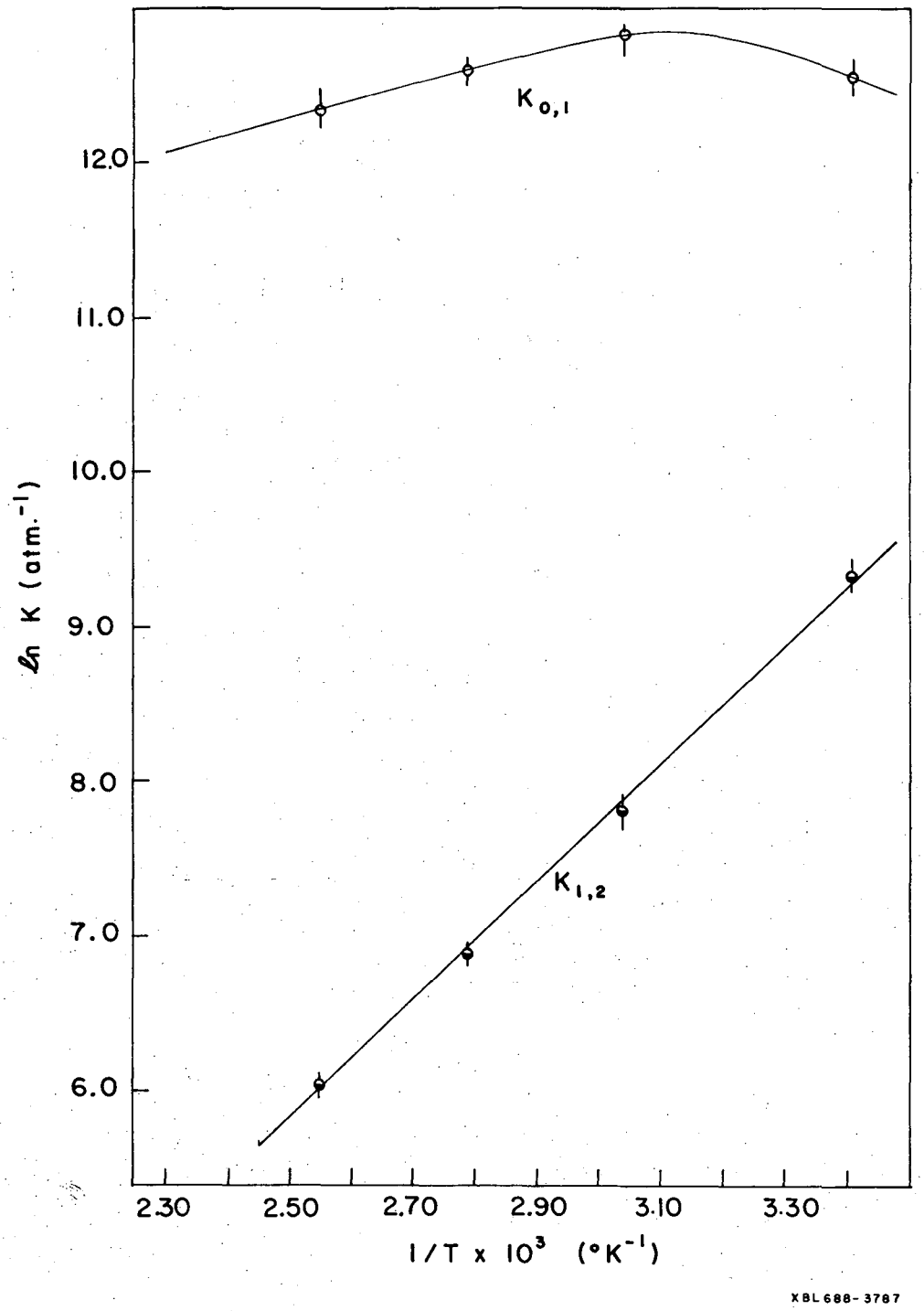

Fig. 17 Temperature dependence of $K_{0,1}$ and $K_{1,2}$ for Series I in mixtures of trimethylamine and helium.

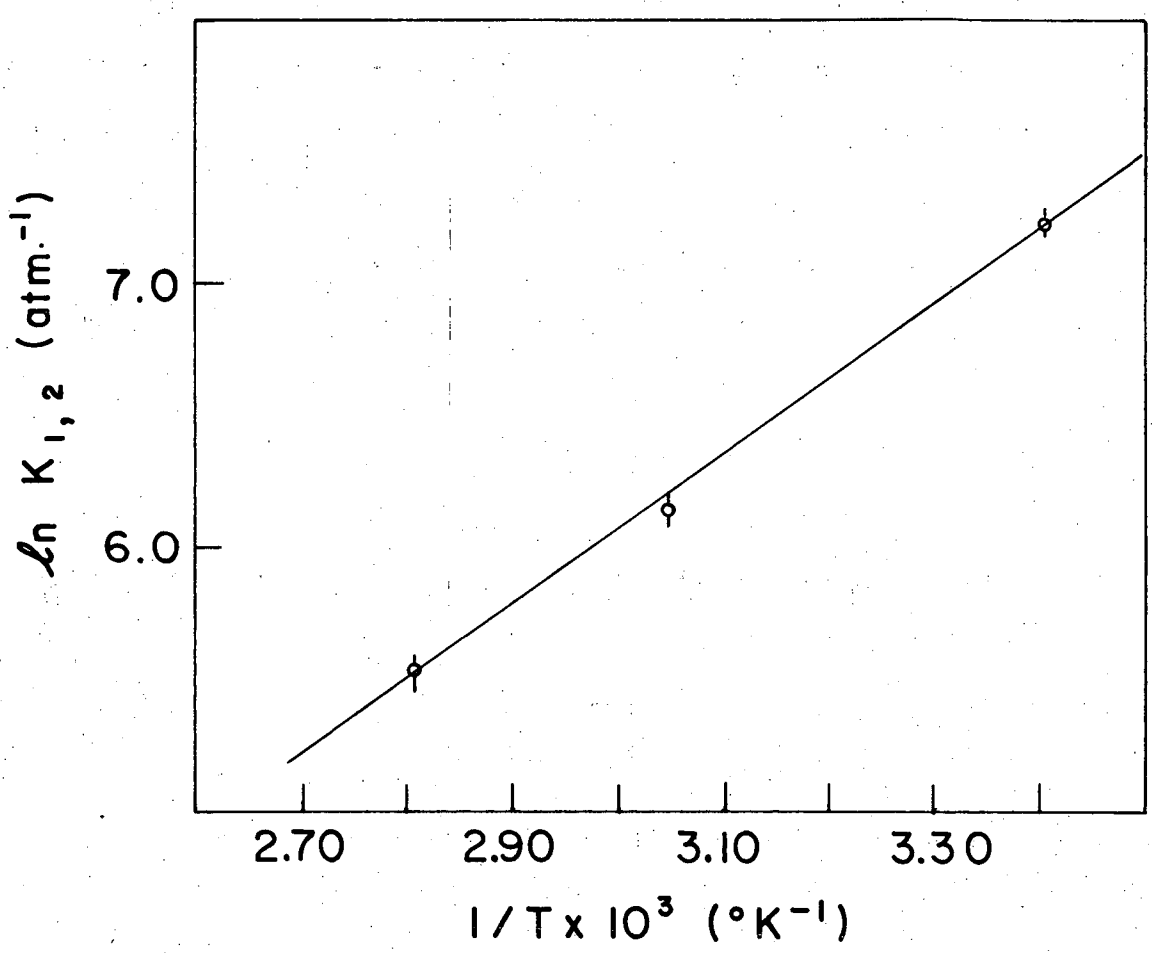

XBL688-3786

Fig. 18 Temperature dependence of $K_{1,2}$ for Series II in trimethylamine.

E. Photoionization of Methylamine

The ions which were detected in the photoionization of methylamine are listed in Table XXIV, where possible chemical identification is suggested. The mass numbers were determined from a calibration obtained from ion signals observed in the photoionization of dimethylamine. Signals below mass 125 are probably accurate to ± 1 mass unit; above mass 125 the inaccuracy increases reaching ± 4 mass units at the highest mass numbers.

At 54.0C in the mixture experiment the intensity of the primary amine ion was large enough to observe at high resolution. The $CH_3NH_3^+$ to $CH_3NH_2^+$ ratio was 2.0. The signal at 63 appeared to be due to just one ion and thus was attributed to $CH_3NH_3^+(CH_3NH_2)$. A signal at 94, the next complex in Series I, was not detected in the temperature range 20.0C to 78.0C. It is possible that the signal at 91, which increases with increasing the temperature, may be covering a weak signal at 94. The signal at 125 was attributed to $CH_3NH_3^+(CH_3NH_2)_3$. When the temperature was raised from 20.0C to 54.0C, it decreased in intensity by a factor of five although there was still no detectable signal at 94. In this situation the temperature dependence of only $K_{0,1}$ can be followed. Typical ion intensities for the (0,1) step are given in Table XXI. Also included are intensities from the other ions observed. Signals above mass 125 were not systematically investigated.

The equilibrium constant for the addition of methylamine to methylammonium ion shows a very weak temperature dependence. The results are given in Table XXVI.

TABLE XXIV

Ionic spectrum of photoionized methylamine

Series I	Mass	Series II	Mass
$CH_3NH_2^+$	31	$(CH_3)_3NH^+$	60
$CH_3NH_3^+$	32	$(CH_3)_3NH^+(H_2O)$	77[a]
$CH_3NH_3^+(CH_3NH_2)_3$	125	$(CH_3)_3NH^+(H_2O)(CH_3NH_2)$	108
		$(CH_3)_3NH^+(CH_3NH_2)_2$	122

Series III	Mass	Series IV	Mass	Series VII	Mass
$(CH_3)_2NN^+(CH_3)_2$	87	147	147	160	160
$87(H_2O)$	105	$147(CH_3NH_2)$	174	$160(CH_3NH_2)$	190
$87(CH_3NH_2)$	119	$147(CH_3NH_2)_2$	202	$160(CH_3NH_2)_2$	216
$87(CH_3)_2NH$	132	$147(CH_3NH_2)_3$	229	$160(CH_3NH_2)_3$	246
$87(H_2O)(CH_3NH_2)$	136				
$87(CH_3NH_2)_2$	150				

[a] The 77 signal was first noticed in the last experiment performed with methylamine and therefore its intensity is not tablulated in Table XXIII.

Table XXV

Temperature dependence of ion intensities in methylamine

Mass	Expt. F[4] 1.24 mmHg amine Temp. 20.0C Intensity(ar. units)	Expt. F[4b] 1.44 mmHg amine Temp. 51.0C Intensity	Expt. F[4c] 1.26 mmHg amine Temp. 77.8C Intensity
31,32[f]	36	31	35
60	42	22	15
63	26	21	19
87	c	42	100
91	55	183	246
105	21	89	b
108	250	340	b
119	400	750	472
122	75	90[a]	c
125	305	110	c
132	125	210	d
135	85	190	
142	254	270	
148	390	218	
160	660	d	
174	107×10^1		
190	109×10^1		
204	860		
219	125×10^1		
233	480		
235	540		
246	510		
261	360		
276	330		

Mass	Expt. H[4] 0.051 mmHg amine 10.10 mmHg helium Temp. 19.0C Intensity (arb.units)	Expt. I[4] 0.055 mmHg amine 9.90 mmHg helium Temp. 54.0C Intensity
31,32[f]	67	63
60	19	22
63	38	33
87	15	80
91	367	790
105	64	235
108	480	280
119	380	390

Table XXV continued

Mass	Expt. H^4 0.051 mmHg amine 10.10 mmHg helium Temp. 19.0C Intensity (arb.units)	Expt. I^4 0.055 mmHg amine 9.90 mmHg helium Temp. 54.0C Intensity
122	275	120[a]
125	200	45[a]
132	185	300
136	253	140[a]
147	e	150
150	360	e
160	400	220
174	240	144
190	138	98
202	d	90
216		56
229		104
246		32

a. A distinct peak can not be detected.
b. Not measured.
c. Not detected.
d. Intensities of higher mass numbers not measured.
e. Peak intensity shifts from 150 to 147 as the temperature was raised.
f. Masses 31 and 32 not resolved

TABLE XXVI

Temperature dependence of $K_{0,1}$ for Series I in methylamine

Expt.	Press.(mmHg) amine	Press.(mmHg) helium	Temp.°(C)	$K_{0,1}(mmHg)^{-1}$
F^{4a}	1.24		20.0	0.54-0.58
F^{4b}	1.44		51.0	0.47-0.53
F^{4c}	1.26		77.8	0.44-0.46
H^{4}	0.051	10.10	19.0	6.08-10.75
I^{4}	0.055	9.90	54.0	5.65- 8.18

VI. THERMODYNAMIC DATA

In Table XXVII we list the thermodynamic data which we have measured and which have been measured by others using the same technique but different ionization sources. We observe that the magnitudes of our enthalpy data are in agreement with that of others. The enthalpies are small, all being less than 1.e.v. This is to be expected for the relatively weak interactions exhibited in a clustering type of reaction.

The entropies we report for the reactions observed in dimethylamine seem reasonable. The large uncertainty in the entropy was due to the uncertainty in the enthalpy to which the entropy is very sensitive. Using statistical mechanics we calculate what might be the maximum entropy change, $\Delta S_{trans.}$, that due to the translational entropy loss when the neutral molecule complexes with the ion. We see that the data imply a net rotation and vibrational increase of about 6 e.u. in reaction (4) and about 10.0 e.u. in reaction (5).

The entropy changes observed in the trimethylamine system seem to be too small when compared to $\Delta S_{trans.}$. We suggest two reasons for this result. The first is that we might expect the enthalpies to be somewhat smaller in the trimethylamine system than in the dimethylamine due to a steric effect; that is, there is present an additional methyl group in the primary ion and in the complexing neutral. This trend is suggested upon comparing reactions (6) and (7) with (4) and (6). The weaker bonds being formed in the trimethylamine system should result in larger net vibration contributions to the entropy change. Secondly, we believe that reactions (6) and (7) correspond to addition of neutral molecules to what is called a closed coordination shell while reaction

(4) corresponds to the completion of a closed shell. This is discussed further in the next section. Neutrals added to a closed shell are expected to be more weakly bound than those of the inner shell. These more freely bound neutrals are expected to provide an additional increase in the rotational and vibrational entropy change.

Table XXVII. Enthalpies and entropies determined from lnK vs. 1/T plots

Reaction	$\Delta H°$(Kcal/mole)	$\Delta S°_T$(e.u.)	$\Delta S°_{Trans}$(e.u.)	Invest
1) $(NH_4^+)(NH_3)_2+NH_3=(NH_4^+)(NH_3)_3$	-12.5 to -13.5 -17.8	-22.4 to -24.8_{294K} -38.0_{298K}	-34.0 -34.0	a b
2) $O_2^+ + O_2 = O_4^+$	-9.68	-20.6_{293K}	-34.2	c
3) $O_2^+ + N_2 = N_2O_2^+$	-5.69±.08	-18.9_{200K}±.4	-32.0	d
4) $(CH_3)_2NH_4^+[(CH_3)_2NH]+(CH_3)_2NH = (CH_3)_2NH_2^+[(CH_3)_2NH]_2$	-11.9 to -13.9 -13.6 to -15.6	-17.3 to -22.3_{294K} e -22.5 to -27.6_{294K} f	-30.1	a
5) $(CH_3)_4N^+[(CH_3)_2NH] + (CH_3)_2NH = (CH_3)_4N^+[(CH_3)_2NH]_2$	-12.2 to -14.1	-20.6 to -26.2_{294K}	-32.7	a
6) $(CH_3)_3NH^+[(CH_3)_3N] + (CH_3)_3N = (CH_3)_3NH^+[(CH_3)_3N]_2$	-7.95 to -9.50	-13.3 to -17.7_{294K}	-37.2	a
7) $(CH_3)_3NH^+[(CH_3)_3N]_2+(CH_3)_3N = (CH_3)_3NH^+[(CH_3)_3N]_3$	-4.07 to -4.83	-3.7 to -6.0_{294K}	-39.4	a
8) $(CH_3)_4N^+[(CH_3)_3N]+(CH_3)_3N = (CH_3)_4^+[(CH_3)_3N^+]_2$	-5.23 to -6.06	-3.60 to -6.20_{294K}	-37.4	a

a-Present work; b-Kebarle, Ref. 9 ; c-Conway, Ref. 3; d-Conway, Ref. 21; e-Ionization with Kr lamp; f-Ionization with Xe lamp.

VII. CONCLUSIONS

One of the initial objectives was to determine the ionic composition of photoionized nitric oxide at pressures in the tenths mmHg range diluted with inert gases in the range 1 to 10 mmHg at room temperature. We can conclude that NO^+ was the only ion of importance under these conditions.

The experiments performed in ammonia were undertaken to prove that the apparatus was capable of detecting complexes. This was affirmed. The data obtained were in fair agreement with that reported by Kebarle.[9] The ammonia in his experiments was ionized with an alpha particle source.

The study of the photoionization of the amines was performed to provide some new information regarding their ionic composition at relatively high pressures. The data taken regarding equilibrium constants were, in general, less than satisfying. The data in the dimethylamine study suggested that the lifetime of the collisionally excited ion $(CH_3)_2NH_2^+$ $[(CH_3)_2NH]_2^*$ was of the order of 10^{-10} sec.

The information obtained in the amine study indicates that the primary amine ions do not completely react with the parent amine to give the ammoniated ion. This is in contrast to the very fast reaction of the ammonia ion with ammonia to give the ammonium ion. However, the mass spectrometric evidence indicated that the ammoniated amine ions were responsible for complexing with the parent amine. This was corroborated by the observation that the addition of one and two neutral molecules respectively to trimethylammonium and dimethylammonium ions produced a closed shell. When the ratio of two equilibrium constants,

$K_{n,n+1}/K_{n+1,n+2}$, is very large, the ionic shell is said to be completed with n+1 neutral molecules. In dimethylamine the ratio $K_{1,2}/K_{2,3}$ was at least 138; in trimethylamine the ratio $K_{0,1}/K_{1,2}$ was 72. One expects the number of neutrals needed to complete a closed shell to be equal to the number of H atoms in the primary ion.

ACKNOWLEDGEMENTS

It is a pleasure to acknowledge the advice and interest which Professor B.H. Mahan contributed to this project.

Special appreciation is extended to the Lawrence Radiation Laboratory machine and glass shops whose craftmanship made possible the fabrication of many complicated assemblies.

I should also like to thank Howard Wood, the director of the Chemistry Department student machine shop, for his helpful suggestions. Many parts of the apparatus were fabricated in his shop.

Consideration is also extended to the varied support facilities of the Inorganic Materials Research Division and to the Lawrence Radiation Laboratory of which it is a part.

This work was performed under the auspices of the U.S. Atomic Energy Commission.

REFERENCES

1. B. H. Mahan and J. C. Person, J. Chem. Phys. 40, 392 (1964).
2. R. N. Varney, ibid. 31, 1314 (1959).
3. J-H. Yang and D. C. Conway, ibid. 40, 1729 (1964).
4. D. C. Conway and J-H. Yang, ibid. 43, 2900 (1965).
5. P. Kebarle and A. M. Hogg, ibid. 42, 798 (1965).
6. A. M. Hogg and P. Kebarle, ibid. 43, 449 (1965).
7. P. Kebarle and A. M. Hogg, ibid. 42, 668 (1965).
8. A. M. Hogg, R. M. Haynes, and P. Kebarle, J.A.C.S. 88, 28 (1966).
9. F. C. Fehsenfeld, K. M. Evenson, and H. P. Broida, Rev. Sci. Inst. 36, 294 (1965).
10. H. Okabe, J. Opt. Soc. Am. 54, 478 (1964).
11. K. Spangenberg and L. M. Field, Elec. Comm. 21, 194 (1943).
12. J. C. Person, Mutual Charge Neutralization of Gaseous Ions, Ph.D. Thesis, University of California, Berkeley, 1963; Lawrence Radiation Laboratory Report, UCRL-10904.
13. W. Paul, H. P. Reinhard and U. von Zahn, Z. fur Physik, Bd. 152, S. 143-182 (1958).
14. K. R. Wilson, Apparatus for Molecular Beam Studies of Chemical Dynamics, University of California, Lawrence Radiation Laboratory Report, UCRL-11605, August 1964.
15. G. W. Goodrich and W. C. Wiley, Rev. Sci. Inst. 32, 846 (1961).
16. P. Kebarle and R. M. Haynes, J. Chem. Phys. 47, 1676 (1967).
17. K. Watanabe, T. Nakayama and J. Mottl, J. Quant. Spectrosc. Rad. Transfer, 2, 369-382.
18. K. Watanabe, J. Chem. Phys. 22, 1564 (1954).

19. E. Tannenbaum, E. M. Coffin, A. J. Harrison, J. Chem. Phys. 21, 311 (1953).

20. G. G. Meisels, Ion Molecule Reactions in the Gas Phase, in Advances in Chemistry, Vol. 58, (American Chemical Society), p. 243, 1966.

21. G. S. Janik and D. C. Conway, J. Phys. Chem. 71, 823 (1967).

This report was prepared as an account of Government sponsored work. Neither the United States, nor the Commission, nor any person acting on behalf of the Commission:

A. Makes any warranty or representation, expressed or implied, with respect to the accuracy, completeness, or usefulness of the information contained in this report, or that the use of any information, apparatus, method, or process disclosed in this report may not infringe privately owned rights; or

B. Assumes any liabilities with respect to the use of, or for damages resulting from the use of any information, apparatus, method, or process disclosed in this report.

As used in the above, "person acting on behalf of the Commission" includes any employee or contractor of the Commission, or employee of such contractor, to the extent that such employee or contractor of the Commission, or employee of such contractor prepares, disseminates, or provides access to, any information pursuant to his employment or contract with the Commission, or his employment with such contractor.